



New morphological and molecular data reveal an important underestimation of species diversity and indicate evolutionary patterns in European *Lepidocyrtus*

Journal:	<i>Invertebrate Systematics</i>
Manuscript ID	IS20016
Manuscript Type:	Research paper
Date Submitted by the Author:	18-Mar-2020
Complete List of Authors:	Mateos, Eduardo; Universitat de Barcelona Facultat de Biologia, Departament de Biologia Evolutiva, Ecologia i Ciències Ambientals Winkler, Daniel; University of Sopron, Faculty of Forestry, Institute of Wildlife Management and Vertebrate Zoology Riutort, Marta; Universitat de Barcelona Facultat de Biologia, Departament de Genètica, Microbiologia i Estadística; Universitat de Barcelona Facultat de Biologia, Departament de Genètica, Microbiologia i Estadística Alvarez-Presas, Marta; Universitat de Barcelona Facultat de Biologia, Departament de Genètica, Microbiologia i Estadística
Keyword:	Collembola, Europe, morphology, phylogeny, species boundaries, species delineation, systematics, taxonomy, DNA bar-coding

SCHOLARONE™
Manuscripts

1 **New morphological and molecular data reveal an important underestimation of**
2 **species diversity and indicate evolutionary patterns in European *Lepidocyrtus***

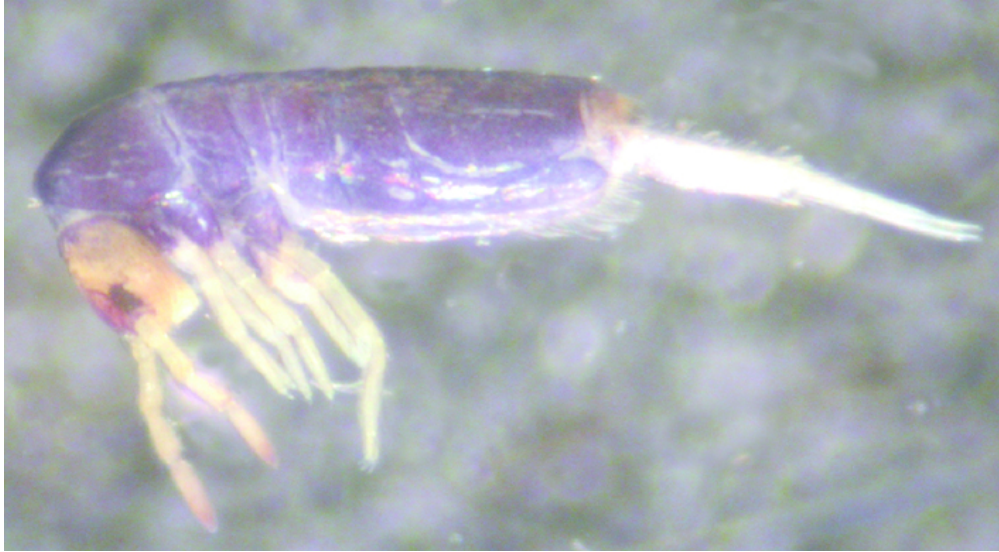
3

4

5 **Short summary**

6

7 Species richness estimation of European Collembola using morphology is challenged
8 by molecular detection of cryptic species. The monophyly of old described
9 *Lepidocyrtus* species and the search for new morphological characters useful for
10 diagnose the detected molecular diversity in this genus is under scrutiny. 26
11 European *Lepidocyrtus* species, including 14 populations of *L. violaceus*, have been
12 morphologically and molecularly studied using sequences of the COXII and EF-1 α
13 genes. Molecular data reveals that the worldwide distributed *Lepidocyrtus violaceus*
14 morphospecies is a polyphyletic entity in Europe. The number and distribution of
15 pseudopores on body and appendages is a promising morphological character with
16 clear phylogenetic signal. As a general trend, an increase in pseudopores number is
17 detected in the evolutive line of the genus *Lepidocyrtus* in Europe.



59x33mm (300 x 300 DPI)

1 **New morphological and molecular data reveal an important underestimation of**
2 **species diversity and indicate evolutionary patterns in European *Lepidocyrtus***
3

4 Eduardo Mateos^{A,B*}, Daniel Winkler^C, Marta Riutort^{D,B} and Marta Álvarez-Presas^{D,B,E}
5

6 ^ADepartament de Biologia Evolutiva, Ecologia I Ciències Ambientals, Facultat de
7 Biologia, Universidad de Barcelona, Spain.
8

9 ^BInstitut de Recerca de la Biodiversitat (IRBio), Universitat de Barcelona, Barcelona,
10 Spain.
11

12 ^CUniversity of Sopron, Faculty of Forestry, Institute of Wildlife Management and
13 Vertebrate Zoology, Sopron, Hungary.
14

15 ^DDepartament de Genètica, Microbiologia i Estadística, Facultat de Biologia,
16 Universitat de Barcelona, Barcelona, Spain.
17

18 ^EUniversity of Bristol, School of Life Sciences, Bristol, United Kingdom

19 *Corresponding author
20

21 Running title: European *Lepidocyrtus* under scrutiny.
22
23

24 Abstract

25

26 The proper identification of morphological species is a key task for species richness
27 estimation of any ecosystem. Although the body colour is a widely used character
28 identifying European *Lepidocyrtus* species, recent investigations using molecular
29 data have revealed that species delineation using body color can result in an
30 underestimation of the real species diversity because of the presence of cryptic
31 species. *Lepidocyrtus violaceus* is a European species characterised by its dark
32 violet body colour. Its wide worldwide distribution leads us to suspect that under this
33 morphospecies several cryptic species can be hidden. Since traditional
34 morphological characters have revealed insufficient for real diversity identification in
35 *Lepidocyrtus*, new morphological characters are needed in order to describe the
36 cryptic diversity detected by molecular data in this genus. Pseudopores are
37 integumentary structures present in all *Lepidocyrtus* species, but the distribution of
38 these structures has not been properly described in the genus. In the present work
39 we aim to analyse whether morphospecies *L. violaceus* is a monophyletic entity in
40 Europe. Moreover, we aim to determine if the position and number of pseudopores in
41 the different parts of the body and appendages is a character with phylogenetic
42 signal useful in the identification of the species or superspecific entities. 14
43 populations of *L. violaceus* from 5 European countries, and another 25 *Lepidocyrtus*
44 species from 9 European countries have been studied. In total 208 specimens have
45 been analysed morphologically and half of them were studied molecularly using
46 sequences of genes COXII and EF-1 α . Molecular data reveals that the worldwide
47 distributed *Lepidocyrtus violaceus* morphospecies is a polyphyletic entity in Europe.
48 Between six and twelve different cryptic species have been detected under the
49 appearance of this European morphospecies, and only the presence of
50 pseudopores on the basal plate of the fourth abdominal segment has been detected
51 as a promising diagnostic character between them. A common basic-pattern of
52 pseudopores distribution has been recognized in the European members of the
53 genus, and also a differential pattern within each European species group. As a
54 general trend, an increase in pseudopores number is detected in the evolutive line of
55 the genus *Lepidocyrtus* in Europe.

56

57 Additional keywords

58 Chaetotaxy, COXII, EF-1 α , cryptic species, DNA, phylogeny, taxonomy,
59 pseudopores.

60

61 **Short summary**

62

63 Species richness estimation of European Collembola using morphology is challenged
64 by molecular detection of cryptic species. The monophyly of old described
65 *Lepidocyrtus* species and the search for new morphological characters useful for
66 diagnose the detected molecular diversity in this genus is under scrutiny. 26
67 European *Lepidocyrtus* species, including 14 populations of *L. violaceus*, have been
68 morphologically and molecularly studied using sequences of the COXII and EF-1 α
69 genes. Molecular data reveals that the worldwide distributed *Lepidocyrtus violaceus*
70 morphospecies is a polyphyletic entity in Europe. The number and distribution of
71 pseudopores on body and appendages is a promising morphological character with
72 clear phylogenetic signal. As a general trend, an increase in pseudopores number is
73 detected in the evolutive line of the genus *Lepidocyrtus* in Europe.

74

75 **Introduction**

76

77 Species richness is usually considered as a proxy of the ecological status of the
78 ecosystems, and "morphological species" is the standard unit of measure for
79 biodiversity purposes. In this context the proper identification of morphological
80 species is a key task for species richness estimation. In soil environments,
81 Collembola is one of the most diverse animal groups, and the estimation of
82 Collembola species richness is important for the assessment of global soil
83 biodiversity.

84 The genus *Lepidocyrtus* Bourlet, 1839 comprises ~250 species (Bellinger et al.
85 1996–2019). Based on chaetotaxy and molecular phylogenetic analysis, European
86 species have been ascribed to five monophyletic groups clearly differentiated by the
87 chaetotaxy (Mateos et al. 2018a), and each group contains unpigmented and
88 pigmented species. Pigment is always dark blue or violet and could be present
89 covering all body (fully-pigmented species) or forming dots or bands in several parts
90 of the body. In both unpigmented and pigmented species pigment is usually present
91 on several parts of the appendages. In all five European species groups at least one

92 fully-pigmented species (or subspecies) is present (see Mateos 2008b, 2011, 2012,
93 Mateos and Petersen 2012, Winkler and Traser 2012). In the present work we deal
94 with *L. violaceus* (Geoffroy, 1762) Lubbock, 1873, the oldest described *Lepidocyrtus*
95 species.

96

97 *Lepidocyrtus violaceus*, a brief history of the oldest species of the genus

98

99 *Lepidocyrtus violaceus* (Geoffroy, 1762) Lubbock, 1873 was originally described as
100 *Podura violacea* Geoffroy, 1762 from specimens from Paris (France). This original
101 description only described the (in French in the original) “purple color a little leaded”
102 as characteristic of the species, without any other morphological description. More
103 than a century later, Lubbock (1873) moved the species to the genus *Lepidocyrtus*
104 and made a brief description accompanied by a picture of a specimen in dorsal view.
105 In the same publication, Beck (1873) described the scales of *L. violaceus* and drew a
106 picture of one of them. Some years later, Parfitt (1891), based on specimens from
107 Exeter (Devonshire, UK), described the pigmentation variability of the species as:
108 “Some are blue, purple, yellowish, bronze-green. Some specimens I collected ... had
109 the head and the last two segments of the body golden-yellow, the rest of the body a
110 splendid purple. Antennae yellow, with the apex of each joint purple. Legs pale
111 yellow.” Sixty five years later, Gisin (1944), based on specimens from Sweden, made
112 another diagnose of the species and described the pigmentation as: (in German in
113 the original) “Blue-violet granulated body. Manubrium and femora (especially femur
114 III) ± purple, without differentiating from body color. Intersegmental bands and dentes
115 clearer. Antennae of uniform violet color, with the antennae bases barely lighter than
116 the head and distal portion of the antennae joints”. Years later Gisin (1964a, 1964b)
117 described the dorsal macrochaetae formula of the head and body (as
118 A0A2A3Pa5/00/0101+3), the basal labium chaetotaxy (as MMRELL, with chaeta R
119 half in length as M chaetae) and the accessory chaetae of anterior trichobothrium of
120 Abd.IV (with chaetae D1, a and m pointed and strongly ciliated). Szeptycki (1967)
121 described the branched morphology of the labral apical chaetae. Based on North
122 American specimens, Snider (1967) described the Abd.III chaetotaxy of dorsal
123 trichobothrial area (were chaeta d3 is absent); Snider also stated that, for years,
124 taxonomists have confused the species *L. violaceus* and *L. cyaneus* Tullberg. Based
125 on specimens from Indiana (USA), Christiansen & Bellinger (1980) described the
126 dorsomedial chaetotaxy of Abd.II–III (Abd.II without chaetae ml and p5p; Abd.III

127 without chaeta d3), and fore foot unguis complex (unguis with basal tooth and two
128 unpaired teeth, empodium lanceolate and with few serrations on the outer edge,
129 tenent hair spatulate); the authors stated that “*it is not certain that Nearctic populations*
130 *are conspecific with European violaceus. ... The general similarity is sufficient to*
131 *justify combinig them for the moment*”. Berg & Heijerman (2002) drew a picture of *L.*
132 *violaceus* from The Netherlands where mesothorax appears not protruding over the
133 head. Mateos (2008a) summarized the available information about the published
134 descriptions of *L. violaceus* (and other European species of the genus), and several
135 authors in recent years have elaborated identification keys where *L. violaceus* is
136 included (Fjellberg 2007, Hopkin 2007, Mateos 2008a, Mateos 2011).

137 It is notorious that, since 1792 different authors have made (partial) descriptions of *L.*
138 *violaceus* based on specimens from different countries and different continents. As a
139 result, *L. violaceus* is nowadays considered a widely distributed species across
140 Europe, Asia, Central and North America, and has also been cited from the Arctic
141 and Antarctic regions (see Bellinger et al. 1996-2019). But, won't *L. violaceus* be a
142 chimera?

143

144 *About body colour and the need for new characters in Lepidocyrtus*

145

146 For centuries, *L. violaceus* has been cited worldwide, and its dark blue pigmented
147 body has always been a key character for its identification. However, DNA-based
148 analyses suggest that the current body colour and morphology-based species
149 delimitation is insufficient for delimiting species in genus *Lepidocyrtus* due to the
150 presence of cryptic species (Zhang et al. 2019a). Thus, the search for new
151 morphological characters, capable of describing the cryptic species that molecular
152 studies are revealing is becoming increasingly necessary.

153 Pseudopores, despite being structures present in most Collembola groups, are
154 usually overlooked in taxonomic descriptions. Only in a few Collembola species the
155 complete distribution of pseudopores on the body has been properly described.
156 Deharveng et al. (2018) presented an overview of pseudopore patterns across
157 Collembola and underlined their interest at different taxonomic level.

158 Pseudopores were described for the first time in Collembola by Gisin (1963). Since
159 this discovery, a pair of dorsal pseudopores from Th.II to Abd.IV and several
160 pseudopores on coxae is known to be characteristic to all Entomobryioidea. One
161 year later, Gisin (1964a) described the presence of pseudopores on each manubrial

162 plate (dorsodistal regions of manubrium) as a characteristic for all Entomobryidae.
163 Since these two referenced Gisin's papers, all *Lepidocyrtus* species descriptions
164 mention the 1+1 dorsal pseudopores from Th.II to Abd.IV, and the 2+2 (rarely 3+3 or
165 4+4) pseudopores on the dorsal manubrial plate, while pseudopores on coxae have
166 been remarked only in a few *Lepidocyrtus* species descriptions (see for example
167 Mateos 2008a, Cipola et al. 2018c).

168 During the postembryonic development of *Lepidocyrtus* (and all Entomobryoidea)
169 chaetotaxy is variable, but the number and position of pseudopores (and also
170 bothriotricha and S-chaetae, see Zhang et al. 2019b) are stable, at least those
171 pseudopores located on the dorsal region of Th.II to Abd.IV, coxae and dorsal
172 manubrial plate. But there is little information about the pseudopores located on other
173 regions of the body, revealing the need to map the complete distribution of
174 pseudopores for taxonomic purposes.

175

176 *The aim of the present work*

177

178 As the base of the present work we have identified 14 European populations of *L.*
179 *violaceus* based on the information currently available for the species, conducting
180 morphological and molecular analysis of these populations and 25 more European
181 *Lepidocyrtus* species (comprising the five groups of European species currently
182 recognised). We are interested in determining whether *L. violaceus* morphospecies
183 corresponds to a monophyletic entity. Taking into account the historical review
184 carried out for this species, we hypothesize a non-monophyletic status for *L.*
185 *violaceus*. For this purpose, we performed a phylogenetic analysis based on two
186 molecular markers (COXII and EF-1 α).

187 With the aim of finding new useful characters for the delineation of the putative
188 cryptic species within *L. violaceus* morphospecies, we have analyzed the distribution
189 of pseudopores on the body of the 14 *L. violaceus* populations. We further have
190 analysed pseudopore number and distribution on the body of the other 25 studied
191 species in order to find some pattern with clear phylogenetic signal at specific or
192 supra-specific level.

193

194 **Material and methods**

195

196 *Specimens*

197

198 Specimens of 14 populations of *L. violaceus* from 5 European countries and another
199 22 described and 3 undescribed *Lepidocyrtus* species from 9 European countries
200 have been analysed morphologically and molecularly (two species were studied only
201 morphologically, see **Table 1**). For molecular analyses 46 specimens of *L. violaceus*
202 and 61 specimens of the other species were studied (**Table 2**). For morphological
203 analyses the skin of the sequenced specimens plus additional 40 specimens of *L.*
204 *violaceus* and 65 specimens of the other species were studied.

205

206 *DNA sequencing, datasets, alignment and phylogenetic tree reconstruction*

207

208 The DNA was obtained with the Speedtools tissue DNA extraction kit (Biotools,
209 Madrid, Spain), following the manufacturer's protocol. The bodies were degraded
210 with proteinase K and the exoskeleton was preserved in 70% ethanol for
211 morphological studies. Polymerase Chain Reaction (PCR) amplification (25 μ L) was
212 performed to obtain a ~800 bp fragment of the mitochondrial cytochrome c oxidase
213 subunit II (COXII) gene and fragments of the first and second exon (~ 500 bp),
214 including an intron of the nuclear EF1- α gene, using the specific primers tRNA-K-
215 LcuJ and tRNA-L-LcuN for COXII, and EFLcuJ and EFLcuN for EF-1 α (Cicconardi et
216 al. 2010). Annealing temperatures of 48 °C and 55 °C for COXII and EF were
217 applied, respectively. Finally, the PCR products were purified using a vacuum
218 manifold (Millipore, SA) and sequenced, using the same primers as in amplification,
219 in Macrogen Europe (Amsterdam, The Netherlands). Chromatograms were revised
220 and contigs constructed in Geneious v 10.2.6. software (Biomatters; available from
221 <http://www.geneious.com>).

222 Three different data sets were used to infer phylogenies, 1) COXII, 2) EF-1 α and 3)
223 Concatenated dataset (with the information of the two genes concatenated). The
224 COXII gene and the coding region of EF-1 α (first and second exons) were aligned
225 following the amino acid pattern with ClustalW tool in BioEdit 7.2.5. (Hall 1999), using
226 the genetic code in table 5 (mitochondrial invertebrate) for the COXII gene and the
227 standard table for EF-1 α gene. The intron of EF-1 α was aligned using MAFFT online
228 version 7 (Kato et al. 2019), and Gblocks 0.91b (Talavera & Castresana 2007) was
229 used to eliminate ambiguously aligned regions or with too many gaps.

230 Version 2.1.1 of PartitionFinder2 (Lanfear et al., 2017) was run on CIPRES Science
231 Gateway (Miller et al. 2010) to identify an appropriate partition scheme and model for

232 each dataset. The data were divided by gene, with unlinked branch lengths, the
233 'raxml' models for selection and the selection criteria under the AICc model with the
234 'greedy' search algorithm. The evolutionary model GTR + G was applied with 8
235 categories for the Gamma distribution, as indicated by the PartitionFinder results. To
236 infer the phylogenies, two different methods were used, Maximum Likelihood (ML)
237 and Bayesian Inference (BI). ML trees were obtained by means of the IQtree
238 software v1.6.1 (Nguyen et al., 2015). IQtree searches were carried out using the
239 program's default configuration, with an initial random tree (option -t RANDOM) and
240 evaluating branch support using 10000 ultrafast bootstrap replicates (Minh et al.
241 2013). Following the results obtained by PartitionFinder, for the analysis of the COXII
242 gene, the first and second position of the codon were separated from the third,
243 however, in EF-1 α all positions were left in the same partition. Each partition was
244 allowed to have its own set of branch lengths (-sp option). To infer phylogenies with
245 the BI method, MrBayes v3.2.6 software was used (Ronquist et al. 2012),
246 establishing the evolutionary model and appropriate partitions according to the
247 results of PartitionFinder with unlinked parameters. Two independent runs of four
248 chains each produced 5 million generations and, for each of them, 5,000 trees were
249 stored. The predetermined 25% value of burnin was used, and it was verified that the
250 probability values (logarithm) of the cold chains reached the stationarity and
251 convergence of the two runs, checking that the average standard deviation of the
252 divided frequencies was lower than 0.1. A consensus tree was obtained from the
253 remaining trees.

254 The FigTree v1.4.4 program (Rambaut 2009) was used to visualize the trees and the
255 iTOL v4 web server (Letunic & Bork 2007) to prepare and generate the tree figures.

256

257 *Species delimitation analysis*

258

259 To confirm the specific hypotheses formulated through the morphological data, a
260 molecular method of species delimitation, ABGD (Puillandre et al. 2012) was applied.
261 The method was implemented through the website
262 <http://wwwabi.snv.jussieu.fr/public/abgd/abgdweb.html>. The COXII dataset was used
263 for this analysis, with the default values of Pmin = 0.001 and Pmax = 0.10, steps = 10
264 and number of intervals = 20. The value of relative gap width value (X) was set at 1.0
265 and was used the correction of K80 Kimura with a MinSlope of 2.

266

267 *Morphological analyses*

268

269 For morphological studies the specimens were mounted on slides with the head
270 separated from the body. The specimens were cleared using Nesbitt fluid and then
271 slide-mounted in Hoyer medium. The slides were studied under a phase contrast
272 microscope with a digital camera attached.

273 Morphological and chaetotaxic characters of the dorsal and ventral regions of the
274 antennae, head, body and appendages were analysed. As a novelty, we studied the
275 basal plate of the fourth abdominal segment (BP4 sensu Hopkin 1997, p. 71), a
276 region of the body that has never been explored in *Lepidocyrtus* until now.

277 Species identification was done consulting the published original descriptions and
278 also the descriptions and identification keys provided by several authors (Fjellberg
279 2007, Hopkin 2007, Mateos 2008a, Mateos 2011).

280 Each species was assigned to a *Lepidocyrtus* group using the diagnostic characters
281 of the European species-groups proposed by Mateos (2008b, 2011, 2012), Mateos
282 and Petersen (2012), and Winkler and Traser (2012).

283

284 *Nomenclature used*

285

286 For the taxonomic descriptions the following terms and codes were used: For dorsal
287 cephalic chaetotaxy the “AMS” nomenclature system (see Soto-Adames 2010). For
288 labial palp Fjellberg (1999). For labial chaetotaxy Gisin (1964b). For interocular
289 chaetotaxy MariMutt (1986). For dorsal chaetotaxy schemes of thoracic and
290 abdominal segments Gisin (1967), Szeptycki (1972, 1979), Wang et al. 2003 and
291 Mateos (2008). For C1–B4/B4–B6 relation on abd. IV Mateos (2008).

292

293 *Abbreviations used*

294

295 The following abbreviations have been used in morphological descriptions: Ant.—
296 antennal segment, Th.—thoracic segment, Abd.—abdominal segment, I–VI—
297 segment numbers, pse—pseudopore, BP4—basal plate of fourth abdominal
298 segment, VT—ventral tube, ret—retinaculum.

299

300 **Results**

301

302 *Molecular analyses*

303

304 *1 - Datasets*

305

306 The COXII dataset, with a final length of 688 bp, comprised 111 sequences from
307 which three corresponded to the selected outgroup (genera *Cyphoderus* and
308 *Orchesella*, Table 2). The EF-1 α dataset, with a final length of 679 bp, included 93
309 sequences (comprising the three outgroups). Finally, the concatenated dataset was
310 composed of 110 specimens (including outgroups) with representation of both genes
311 in almost all of them (see Table 2) with a final length of 1367 bp.

312

313 *2 - European groups*

314

315 In the phylogeny inferred using the concatenated dataset (Figs. 1 and 2), the five
316 European *Lepidocyrtus* species groups were recovered with both methods used (ML
317 and BI) as monophyletic groups with high support (only *pallidus*–*serbicus*-group does
318 not have high support in either method, although it is monophyletic in both, Fig. 1).
319 The most basal clade (Fig. 1) was *lusitanicus*-group (sensu Mateos 2008b), including
320 *L. bilobatus* Mateos, 2008, *L. lusitanicus* Gama, 1964 and *L. selvaticus* Arbea &
321 Ariza, 2007 specimens. The *lanuginosus*-group (sensu Mateos 2011) clade included
322 *L. bicoloris* Mateos, 2012, *L. cyaneus* Tullberg, 1871 and *L. lanuginosus* (Gmelin,
323 1788) specimens. The clade *pallidus*–*serbicus*-group (sensu Gisin 1965; Winkler and
324 Traser 2012) included *L. arrabonicus* Traser, 2000, *L. pallidus* Reuter, 1890 and *L.*
325 *serbicus* Denis, 1933 specimens. The *curvicollis*-group (sensu Mateos and Petersen
326 2012) clade consisted of the *L. flexicollis* Gisin, 1965, *L. montseniensis* Mateos, 1985
327 and *L. paradoxus* Uzel, 1890 specimens, and formed the sister group to the clade
328 comprising the *lignorum*-group (sensu Mateos 2011) (Fig. 2), that included *L.*
329 *barbulus* Mateos, 2011, *L. chorus* Mateos & Lukić, 2019, *L. intermedius* Mateos et al.
330 Mateos, Escuer & Álvarez-Presas, 2018, *L. juliae* Mateos, 2011, *L. lignorum*
331 (Fabricius, 1793), *L. pulchellus* Denis, 1926, *L. spJ*, *L. spK*, *L. spL*, *L. tellecheae*
332 Arbea & Jordana, 1990, *L. traseri* Winkler, 2016, and *L. violaceus*. The species
333 *Lepidocyrtus* spJ, spK, and spL are still under study, but their morphological
334 characters perfectly comply with the definition of the *lignorum*-group. Within this
335 *lignorum*-group clade, the 14 *L. violaceus* populations were grouped into six main
336 lineages (Fig. 2). These main *violaceus* lineages have been coded with capital letters

337 and numerical subindexes from A1 to G, each capital letter grouping specimens from
338 nearest geographical locations.

339 ABGD molecular species delimitation analysis defines 39 putative entities
340 (=molecular entities) (Figs. 1 and 2), from which 12 correspond to the *violaceus*
341 lineages inferred in the tree (Fig. 2). The specimens morphologically identified as *L.*
342 *arrabonicus* (within the *pallidus*–*serbicus* group, Fig. 1), *L. lignorum*, *L. spK* and *L.*
343 *violaceus* (within *lignorum*-group, Fig. 2) did not form a monophyletic entity, indicating
344 the presence of cryptic species. The monophyletic subgroup within the *lignorum*-
345 group formed by the molecular entities *violaceus* G, *juliae*, *lignorum*-1, and spL share
346 the synapomorphy of the presence of pseudopores on the BP4. No other studied
347 specimens have pseudopores on this region of the body.

348

349 3 - *Lepidocyrtus violaceus*

350

351 Geographical proximity appears as a key element grouping the 12 molecular entities
352 within the six main *violaceus* lineages (see Fig. 3). All populations in cluster A
353 (including molecular entities *violaceus* A1, *violaceus* A2 and *violaceus* A3) were
354 distributed in Pyrenean localities, in Northeastern Spain. Populations in cluster B
355 (with molecular entities *violaceus* B1, *violaceus* B2 and *violaceus* B3) were located in
356 Western Iberian Peninsula, near the border between Spain and Portugal. Population
357 in cluster C (including molecular entities *violaceus* C) was located also in Western
358 Iberian Peninsula, in the vicinity of Coimbra city (Portugal). The two populations in
359 cluster D (including molecular entities *violaceus* D) have a close distribution (a few
360 kilometres away) in the “Serra de Prades” mountains (Spain). Population in cluster E
361 (including molecular entities *violaceus* E) was located in Italy. Populations in cluster F
362 (including molecular entities *violaceus* F1 and *violaceus* F2) were placed in Hungary.
363 Population in cluster G (including molecular entities *violaceus* G) was located in
364 Moldova.

365

366 Systematics

367

368 Family *Entomobryidae* Schott

369

370 Genus *Lepidocyrtus* Bourlet

371

European *Lepidocyrtus* species groups

(Figs. 1, 4 – 11, Tables 1 – 3)

372

373

374

375 We have revised the number and position of pseudopores on all *Lepidocyrtus*
376 species included in the present work. Pseudopores were present in 33 positions
377 including coxae, dorsal head, dorsal and ventral body, ventral antennae, dorsal
378 manubrium and dorsal dentes. We have detected the presence of a basic common
379 scheme of pseudopores distribution for all species, and also a differential scheme for
380 several European species groups. **Table 3** summarizes the number of pseudopores
381 present on each position for all studied species. In the following paragraphs the
382 different positions where pseudopores have been detected are described.

383 On the legs, pseudopores are located on the external face of the three coxae
384 (positions 1 – 3). On Cx.I 2 pseudopores is the common number in all species except
385 for *L. selvaticus* (with only one). On CX.II the number of pseudopores varies between
386 2 and 8 depending on species and species groups, and when more than three
387 pseudopores are present the rest have smaller size. On CX.III always 2 pseudopores
388 are present in all studied species.

389 On the head, pseudopores are located in two positions of the periantennal area on
390 the anterior end (positions 4 and 5, **Fig. 4**, and always in the same number: 1+1
391 externally to antennal basis, and 2+2 internally to the antennal basis. These 2+2
392 pseudopores located between antennal bases are very difficult to observe because of
393 the stacking of chaetae that occurs in microscopic slides.

394 On the dorsal region of the body 1+1 pseudopores in mid dorsal position from Th.II to
395 Abd.IV are always present (positions 6 – 11); other pseudopores on dorsal Abd.IV
396 (position 12) were present only in one species (*L. curvicollis*).

397 On the furca, pseudopores are located on the dorsal region of manubrium and
398 dentes. On the manubrium, 1+1 pseudopores in dorsobasal region (position 13, **Fig.**
399 **5**) and 2-3+2-3 in dorsodistal region (2-3 on each manubrial plate, position 14) are
400 always present. On the dentes, when present, pseudopores are disposed on
401 dorsobasal region (position 15) and, when there is more than one, they are disposed
402 forming a row one behind the other from the base towards the apical end.

403 On the antennal joints I – III (positions 16 – 18), pseudopores, when present, are
404 always located ventrally on the apical membranous area (**Fig. 6**), between the apical
405 row of chaetae and the tip of the joint.

406 On the ventral region of the thorax 1+1 pseudopores from Th.I to Th.III (near coxae)
407 are always present (positions 19 – 21). On the ventral region of the abdomen 1+1
408 pseudopores anterior to the ventral tube (position 22) and 1+1 posterior to the ventral
409 tube (position 23) (on Abd.I) are always present; also at least 2 pseudopores on
410 Abd.II (position 24, between ventral tube and retinaculum, Fig. 7), 2 on Abd.III
411 (position 25, in a linear disposition posterior to retinaculum, Fig. 8), and 1 on Abd.V
412 (position 27, anterior to genital plate, Fig. 5). On the ventral region of Abd.IV,
413 pseudopores are only present on several species of *curvicollis*-group, located
414 internally to BP4 (position 26).

415 On the lateral region of the body, pseudopores are only present on *L. mariani*, with
416 many small (compared to dorsomedial ones) pseudopores from Th.III to Abd.IV
417 (positions 28 – 32). On four molecular entities of *lignorum*-group pseudopores are
418 located on the BP4 (position 33), these species are *L. juliae* with 10 pseudopores on
419 BP4, *L. lignorum-1* with 6 pseudopores, *L. spL* with 4 – 6 pseudopores, and *L.*
420 *violaceus* G with 7 pseudopores. All four mentioned species form a monophyletic
421 group in the concatenated tree (Fig. 2).

422 The outgroup *Cyphoderus* cf. *bidenticulati* has pseudopores located in the same
423 positions as *Lepidocyrtus* species (Table 3), with only two main differences:
424 presence of 3 pseudopores located behind the posterior row of chaetae on the
425 dorsum of Abd.IV (position not coded, see Deharveng et al. 2018), and absence of
426 pseudopores on the manubrial base (position 13). No data available on the
427 distribution of pseudopores in the genus *Orchesella*.

428

429 *Remarks*

430

431 As is shown in Table 3, several positions of the body and apendages have a fixed
432 number of pseudopores on all studied species (positions marked with asterisk in
433 Table 3), while other regions show within-groups and between-groups variability. In
434 Figs 9 and 10 pseudopores on dorsal, lateral and ventral positions are mapped for
435 the five European species groups of *Lepidocyrtus*, indicating the variability observed
436 on the different positions.

437 *Lusitanicus*-group and *Ianugiosus*-group are characterised by the absence of
438 pseudopores on dorsal dentes and ventral Ant.II (positions 15 and 17). *curvicollis*-
439 group is characterised by the presence of pseudopores on ventral Ant.I (position 18).

440 Abd.IV is a region where pseudopores can be present in different positions
 441 depending on the species or species groups. In this segment, all species have the
 442 1+1 dorsomedial pseudopores in position 11; in dorsolateral position 12 only species
 443 *L. curvicollis* (from the *curvicollis*-group) has a group of 5 – 7 pseudopores; on ventral
 444 position 26 only the species *L. flexicollis*, *L. mariani* and *L. montseniensis* (from the
 445 *curvicollis*-group) have several pseudopores; on lateral position 32 only the species
 446 *L. mariani* (from *curvicollis*-group) has pseudopores; and on lateral position 33 the
 447 four molecular entities *L. lignorum*-1, *L. juliae*, *L. violaceus* G, and *L. spL* (from
 448 *lignorum*-group) have several pseudopores on BP4 (Fig. 11).

449

450 ***Lepidocyrtus violaceus*** (Geoffroy 1762) Lubbock 1873

451 (Figs. 2, 3, 12 – 15, Tables 1, 2, 4, 5)

452

453 *Diagnosis*

454

455 Uniform violet body color on dorsal and ventral surfaces from Th.II to Abd.IV, Abd.V–
 456 VI, head and manubrium with or without pigment, legs with pigment on coxae, hind
 457 legs also with pigment on trocanter and femur (see pictures on Fig. 2). Mesothorax
 458 slightly projected over the head. Ant.I–II, legs and dorsal side of manubrium scaled.
 459 Labium chaetotaxy M1M2REL1L2 (R half in length than M chaetae). Labral chaetae
 460 formula 4/554; prelabral chaetae ciliated; apical row of labral chaetae branched.
 461 Dorsal macrochaetae formula A0A2A3Pa5/00/0101+3. On dorsal head the short
 462 macrochaeta A2a is present in front of macrochaeta A2. On Abd.II the dorsal
 463 macrochaeta is m3, on Abd.IV dorsal macrochaetae are C1+B4, B5, B6. Ungues with
 464 paired basal teeth, one sub-equal median tooth, and a tiny apical tooth. Unguiculi
 465 lanceolate, with denticles along outer edge.

466 The pseudopores number and position in all the specimens studied are as follows
 467 (Table 4, Fig. 12):

468 Legs: 2 on Cx.I; 4 on Cx.II; 2 on Cx.III.

469 Head: 1+1 located anteriorly to each eye patch (dorsoexternally to Ant.I), and 2+2
 470 located dorsointernally to each Ant.I.

471 Dorsal body: 1+1 on each segment from Th.II to Abd.IV (near the central axis of the
 472 segments).

473 Furca: 1+1 on dorsal manubrial base; 2 on each dorsal manubrial plate; 3 on each
 474 dorsal dentes base.

475 Antenna: 1 on ventral side of Ant.II and Ant.III, located distally on the membranous
476 area between the chaetae of the apical row and the tip of the antennal joints.

477 Ventral body: 1+1 on each thoracic segment (near the base of coxae), 1+1 anteriorly
478 to the base of the ventral tube and 1+1 posteriorly to the base of the ventral tube, 3 –
479 4 forming a triangle or a rectangle between ventral tube and retinaculum, 2 in a line
480 posterior to retinaculum, and 1 anterior to genital plate on Abd.V.

481 Lateral body: Lateral pseudopores only presents in population *L. violaceus*_392, with
482 7 pseudopores located on BP4.

483

484 *Remarks: Intrapopulational and intraindividual variability*

485

486 Although all the specimens labelled as *L. violaceus* match the species diagnosis,
487 variability in the presence/absence of some chaetae or pseudopores has been
488 detected in some populations. Also, bilateral asymmetries in several specimens have
489 been observed. This variability affects the interocular chaeta q, Abd.II chaetae ml and
490 p5p, Abd.III chaetae mi and d3, Abd.IV ratio B4-B5/B5-B6, development of
491 macrochaeta B6 on Abd.IV, and presence/absence of pseudopores on BP4. This
492 variability is summarized in **Table 5** and described in the following paragraphs.

493 - Interocular chaeta q (**Fig. 13**) is absent in all specimens, but in the population
494 *L.violaceus*_539 two specimens have asymmetric interocular chaetotaxy, with chaeta
495 q present only on one ocular area.

496 - Abd.II chaeta ml (associated with trichobothrium m2, **Fig. 14-a**) is absent in ten
497 studied populations, present in two populations, and present or absent in two
498 populations. On population *L.violaceus*_457 one specimen has asymmetric
499 chaetotaxy with ml present only on one side of the body.

500 - Abd.II chaeta p5p (**Fig. 14-b**) is present in four populations, absent in eight
501 populations, and present or absent in two populations. In population *L.violaceus*_539
502 three specimens have asymmetric chaetotaxy with p5p present only on one side of
503 the body.

504 - Abd.III chaeta mi (associated with trichobothrium m2) is present in two populations,
505 absent in nine populations, and present or absent in three populations. In population
506 *L.violaceus*_539 one specimen has asymmetric chaetotaxy with chaeta mi present
507 only on one side of the body.

508 - Abd.III chaeta d3 (**Fig. 15**) is present in ten populations and absent in four
509 populations.

510 - On Abd.IV the ratio B4-B5/B5-B6 is <1.6 in six populations (inner rectangle in Fig.
511 15) and >2 in eight populations (outer rectangle in Fig. 15). In the specimens with
512 ratio <1.6 Abd.IV macrochaetae B4, B5 and B6 are of the same shape (broad ciliated
513 macrochaetae), while in specimens with ratio >2 Abd.IV chaeta B6 is a thin ciliated
514 macrochaeta, with a reduced socket respect to macrochaetae B4 and B5. Gisin
515 (1964a) described the species *L. violaceus* indicating that macrochaetae B5 and B6
516 on Abd.IV are close to each other, and B6 is thinner and acuminate.

517 - BP4 pseudopores are only present in population *L. violaceus*_392, with seven
518 pseudopores on each side of the body (Fig. 12).

519 With this variability observed in the 14 populations of *L. violaceus* it is not possible to
520 diagnose the 12 molecular entities detected by the ABGD analysis. Only the
521 presence of pseudopores on BP4 in the specimen *L. violaceus*_392, defined as
522 molecular entities *violaceus* G, can be considered a diagnostic character defining this
523 species.

524

525 **General discussion**

526

527 *Subgenera and species groups in European Lepidocyrtus*

528

529 The species analysed in the present study cover all the five European species
530 groups of *Lepidocyrtus* currently recognized. Also, the two subgenera of *Lepidocyrtus*
531 present in Europe are represented, *Lanocyrtus* Yoshii & Suhardjono, 1989 and
532 *Lepidocyrtus* s. str. Yosii, 1959. As in Mateos et al. (2018a), our results suggest that
533 subgenus *Lanocyrtus* (including species groups *lusitanicus*, *lanuginosus* and
534 *pallidus-serbicus*) is a non-monophyletic group, whereas *Lepidocyrtus* s. str.
535 subgenus (including species groups *lignorum* and *curvicollis* as sister groups) is a
536 monophyletic group. The presence of scales on antennae and legs beyond coxae are
537 the main morphological characters diagnosing the species groups included in
538 *Lepidocyrtus* s. str. subgenus, and within this subgenus, *curvicollis*-group is
539 characterizaed by the presence of chaeta "s" on Abd.IV (Mateos et al. 2018a). Our
540 results suggest that the presence of pseudopores on the ventral apical region of Ant.I
541 is another diagnostic character of the species included in the *curvicollis*-group.

542

543 *About pseudopores in Lepidocyrtus and other Entomobryoidea*

544

545 We strongly agree with the comment of Deharveng et al. (2018) stating that
546 “Evidence is therefore increasing that these tiny pseudopores have diversified
547 distribution patterns that provide (or may provide) powerful characters at all
548 taxonomic levels.” But published information dealing with pseudopores number and
549 position in Entomobryoidea are scarce, and in no case the complete mapping of
550 these structures has been described for any species.

551 With the current published information, it is not possible to know the stability of the
552 number and position of pseudopores in *Lepidocyrtus* (and in Collembola in general)
553 during postembryonic development. For example, in *Lepidocyrtus mariani* Mateos &
554 Winkler (2018) found that the number of small dorsolateral pseudopores located on
555 Th.III to Abd.IV is variable depending on the size of the specimen. The information
556 currently available about pseudopores in *Lepidocyrtus* and other Entomobryoidea is
557 presented below.

558

559 **Legs:** Coxal pseudopores are known in Collembola since Gisin (1963), who
560 described the presence of this structure on Cx.I – II in several genera of
561 Entomobryidae, including *Lepidocyrtus*. Subsequently, pseudopores on Cx.I – III
562 have been described in many Entomobryoidea genera: *Acanthocyrtus* (Cipola et al.
563 2018a), *Amazhomidia* (Cipola et al. 2016a), *Campylothorax* (Santos et al. 2016,
564 Bellini & Cipola 2017), *Coecobrya* (Cipola & Bellini 2016, Jantarit et al. 2019),
565 *Cyphoderus* (Nunes & Bellini 2018), Entomobrya (Ma & Shi 2018), *Heteromurus*
566 (Lukić et al. 2015), *Homidia* (Pan et al. 2015), *Lepidocyrtoides* (Cipola et al. 2017),
567 *Lepidonella* (Deharveng et al. 2018), *Troglobius* (Cipola et al. 2016b), *Trogolaphysa*
568 (Bellini & Cipola 2017, Nunes & Bellini 2018), *Seira* (Cipola et al. 2018b), and
569 *Tyrannoseira* (Cipola et al. 2019). In all cited genera Cx.II is where the number of
570 pseudopores is more variable, as is the case described in the present work for position
571 2.

572

573 **Head:** Hütner (1986) described in *Lepidocyrtus* the presence of the “antennobasal-
574 organ” as a “small deep groove seeing with the light microscope” and located on the
575 external face of each Ant.I base. In our opinion this “antennobasal-organ”
576 corresponds to the pseudopore described for *Lepidonella doveri* by Deharveng et al.
577 (2018) as those “located externally to antennal basis on head in the periantennal
578 area”. This structure represents the 1+1 dorsal head pseudopores, located externally

579 to antennal basis on the periantennal area, described in the present work in position
580 4.

581 Winkler & Traser (2012) described the presence of two pseudopores on the inner
582 side of each antennal base in *Lepidocyrtus tomosvaryi*; the same number and
583 position of pseudopores have been described by Winkler (2016, 2017) for *L. traseri*
584 and *L. isabellae* respectively, and by Mateos & Winkler (2018) for *L. floriae*. These
585 pseudopores correspond to the 2+2 anterointernal pseudopores located on the
586 periantennal area described in the present work in position 5 for all studied
587 *Lepidocyrtus* species. Jantarit et al. (2014) described in *Cyphoderus* (and they say
588 “for the first time in Collembola”) the presence of 1 or 2+2 pseudopores on head
589 anteriorly to the antenno-basal line (position 5), and Jantarit et al. (2019) described
590 the presence of 1+1 pseudopores on this position in *Coecobrya sirindhornae*.

591

592 **Dorsal body:** In *Lepidocyrtus* (and all Entomobryoidea) 1+1 dorsal pseudopores
593 from Th.II to Abd.IV are always present, and represent those described from position
594 6 to position 11 in the present work. Pseudopores located on other positions of dorsal
595 body in the genus have been only described for *L. curvicollis* (see Mateos 2008a),
596 with its characteristic 5–7+5–7 pseudopores on dorsal Abd.IV in position 12.

597 Cipola et al. (2018b) described the presence of 10 pseudopores on the anterior
598 region of dorsal Abd.IV in *Seira baetica*, and several pseudopores on the dorsolateral
599 region of Th.III – Abd.III (with 10, 11, 3 and 12 pseudopores on each segment
600 respectively) in *Seira burgersi*; the authors stated that the presence of pseudopores
601 on anterior and dorsolateral regions of thoracic and abdominal segments is an
602 exclusive feature registered for the first time in *Seira*. Deharveng et al. (2018)
603 indicated that the presence of several pseudopores behind the posterior row of
604 chaetae on the dorsum of Abd.IV is a synapomorphy of the group formed by
605 Troglopedetinae + Cyphoderidae, separating them from other Paronellidae and
606 Entomobryidae.

607

608 **Furca:** The presence of pseudopores on dorsobasal position of manubrium in the
609 genus *Lepidocyrtus* has been only described by Winkler & Traser (2012), who noted
610 the presence of 3 pseudopores (forming a triangle) on this position in species *L.*
611 *tomosvaryi*. Likewise, Deharveng et al. (2018) described the same number and
612 position of pseudopores in dorsobasal region on manubrium (3, forming a triangle
613 near the genital plate) in *Lepidonella doveri*. We consider that these 3 pseudopores

614 forming a triangle described for *L. tomosvaryi* and *L. doveri* are actually 1+1 on
615 dorsobasal manubrium (position 13) and 1 (odd) on ventral Abd.V located anterior to
616 genital plate (position 27, see Fig. 5). Also in *Coecobrya xui* the presence of 2
617 pseudopores has been described on dorsobasal position of manubrium on position
618 13 (Zhang & Dong 2014).

619 The presence of pseudopores on the manubrial plate (dorsodistal region of
620 manubrium, position 14) in *Lepidocyrtus* is largely described for all species since its
621 detection by Gisin (1964a). In all Entomobryidae species the usual number of
622 pseudopores in this position is 2–3+2–3, but in *Verhoeffiella* 4–14 has been
623 described as a usual number (Lukić et al. 2015). This high number of pseudopores
624 on the apical dorsal region of manubrium is considered taxonomically important by
625 Lukić et al. (2018).

626 In *Tomocerus* the presence of a large number of dorsal pseudopores (up to 27+27)
627 on each side of the manubrium seems to be a general rule (see Yu et al. 2014).
628 Pseudopores on this area of the manubrium have not been detected so far in other
629 Entomobryomorpha.

630 In *Lepidocyrtus* the presence of pseudopores on the basal region of dorsal dentes
631 (position 15) has been only described by Winkler & Mateos (2018) in the species *L.*
632 *mariani*. Deharveng et al. (2018) also cited the presence of pseudopores on this
633 position, saying verbatim “new location, observed in many Entomobryidae”, but
634 without indicating any specific case.

635

636 **Ventral body:** In *Lepidocyrtus* the presence of pseudopores on the ventral region of
637 the body has been described only in a few species. Deharveng et al. (2018) cited that
638 the presence of pseudopores between tenaculum and ventral tube has been
639 observed in *Lepidocyrtus* sp. and *Cyphoderus* sp., but without indicating any specific
640 case. For *Lepidocyrtus mateosi* Cipola et al. (2018c) described the presence of 1+1
641 basal pseudopores on the anterior region of the corpus of the VT. On other
642 Entomobryoidea pseudopores on the corpus of VT have been described for
643 *Tyrannoseira* as 1+1 on the base of the anterior region (Cipola et al. 2019), and for
644 *Sinella abietis* as 1+1 on the middle of the anterior part (Ding & Zhang 2015). On
645 other ventral regions of the body pseudopores have never been formally described
646 for any Entomobryoidea. So the presence in *Lepidocyrtus* of 1+1 pseudopores on the
647 ventral region of Th.I to Th.III on positions 19 to 21 (near the coxae bases), 1+1 on
648 positions 22 and 23 (anterior and posterior base of VT), 3 – 5 on position 24

649 (between the base of VT and retinaculum), a pair (forming a line) on position 25
650 (posterior to retinaculum), and several on position 26 (ventral Abd.IV) on several
651 species of the *curvicollis*-group, are formally described for the first time in Collembola
652 in the present work.

653

654 **Antenna:** In *Lepidocyrtus* the presence of pseudopores on the ventral region of Ant.I
655 – III joints has only been described for the species *L. mariani* (Winkler & Mateos
656 2018). These pseudopores are located distally on the membranous area between the
657 tip of the antennal joints and the chaetae of the apical row (positions 16, 17 and 18),
658 and their presence on all *Lepidocyrtus* species is stated for the first time in the
659 present work.

660 Also the presence of ventral antennal pseudopores has been described on Ant.I – III
661 for the genera *Coecobrya* (Jantarit et al. 2019), *Dicranocentrus* (Ren et al. 2018) and
662 *Verhoeffiella* (Lukić et al. 2015, 2018), on Ant.II – III for genera *Cyphoderus* (Jantarit
663 et al. 2014) and *Lepidonella* (Deharveng et al. 2018), and on Ant.III for the genus
664 *Paronella* (Barra 1969). The highest number of pseudopores on antennal joints is
665 found in *Verhoeffiella* (Lukić et al. 2018), specially on Ant.II with a maximum of 15.

666

667 **Lateral boby:** In genus *Lepidocyrtus* the presence of pseudopores on the lateral
668 regions of the body has been described in a few occasions. Mateos & Greenslade
669 (2015) described the presence of two pseudopores on lateral Abd.IV (along the
670 suture tergum-BP4, position 32) for several species of *Setogaster* subgenus. Cipola
671 et al. (2018c) described the presence of dorsolateral pseudopores on Th.II–III (2
672 pseudopores on each segment) and Abd.III (5 pseudopores) in *Lepidocyrtus*
673 *amazonicus*. Winkler & Mateos (2018) described the presence of numerous small
674 pseudopores on dorsolateral regions of Th.III to Abd.IV (positions 28 to 32) in
675 *Lepidocyrtus mariani*. For other Entomobryoidea only Deharveng et al. (2018)
676 described the presence of pseudopores on lateral Abd.IV along the suture tergum-
677 BP4 in *Lepidonella doveri*. The presence of lateral pseudopores on the BP4 (position
678 33), found in four *Lepidocyrtus* populations from the lignorum-group in the present
679 work, is here described for the first time for Entomobryoidea. Interestingly, these
680 populations with pseudopores on BP4 (*L. violaceus* G, *L. juliae*, *L. spL* and *L.*
681 *lignorum*-1) are grouped forming a monophyletic group in the concatenated
682 phylogeny (Fig. 2), suggesting a phylogenetic signal for the presence of these
683 pseudopores.

684

685 *Cryptic species*

686

687 The 14 populations of *L. violaceus* studied perfectly comply with the currently
688 morphological diagnosis proposed for this species. But within these morphospecies,
689 phylogenetic analyses showed six (non-sister groups) main clusters, and ABGD
690 analysis showed twelve putative molecular (cryptic) entities. The morphological study
691 has not detected any character that allows a differential diagnosis for each of these
692 main clusters nor for the putative molecular entities. Only the presence of
693 pseudopores on BP4 in specimen *L. violaceus*_392_2 is a differential character for
694 the molecular entities *L. violaceus* G (Figure 2). This scenario is congruent with the
695 presence of 6 to 12 cryptic species within the European morphospecies *L. violaceus*.
696 The existence of distinct lineages/cryptic species in the genus *Lepidocyrtus* has been
697 detected in several studies using molecular data (Cicconardi et al. 2010; 2013;
698 Mateos et al. 2018; Zhang et al. 2018a; 2019a), and also other studies suggested
699 their existence in several groups of Collembola (Katz et al. 2015; Anslan and
700 Tedersoo 2015; Nilsai et al. 2017; Zhang et al. 2018b). Results of all these studies
701 (and the present study) suggest that sampling additional locations and/or habitats
702 would reveal even more lineages/cryptic species in Collembola. With the data
703 presented in this work, it is not possible to diagnose any of the molecular entities as
704 new species, which would have to be analysed more deeply at the morphological
705 level. We can consider, then, such molecular entities as Unconfirmed Candidate
706 Species (UCS).

707

708 **Conclusions**

709

710 Molecular data reveal that the worldwide distributed *Lepidocyrtus violaceus*
711 morphospecies is a polyphyletic entity. Between six and twelve different cryptic
712 species have been detected in Europe under the appearance of this
713 morphospecies. This indicates that the true diversity of Collembola can be strongly
714 underestimated if only traditional morphological characters (including body colour)
715 are used for the identification of the species. The results obtained in the present
716 paper suggest that the number and position of pseudopores on the body and
717 appendages are promising useful diagnostic characters for species or species-
718 groups identification in European *Lepidocyrtus*. Species of the *Iusitanicus*-group and

719 *lanuginosus*-group, in a phylogenetic basal position within the European
720 *Lepidocyrtus*, have the most basic scheme of pseudopores distribution, indicating an
721 increase in pseudopores number in the evolutive line of the genus *Lepidocyrtus* in
722 Europe. Our results suggest that the current richness of Collembola species in
723 Europe is underestimated.

724

725 **Acknowledgments**

726

727 We are very grateful to Alba Enguíanos and Gema Blasco for the molecular work
728 carried out in the laboratory.

729

730

731 **Conflicts of Interest**

732

733 The authors declare no conflicts of interest.

734

735

736 **References**

737

- 738 Anslan, S., and Tedersoo, L. (2015). Performance of cytochrome c oxidase subunit I
739 (COI), ribosomal DNA Large Subunit (LSU) and Internal Transcribed Spacer 2
740 (ITS2) in DNA barcoding of Collembola. *European Journal of Soil Biology* 69, 1–7.
- 741 Barra, J.A. (1969). Collemboles du Gabon. *Revue Biologia Gabonica* 5, 189-216.
- 742 Beck, J. (1873) Essay on the scales of the Collembola and Thysanura.
743 In 'Monograph of the Collembola and Thysanura'. (Ed Lubbock, J.) pp. 249–254.
744 (J. Ray Society, London).
- 745 Bellinger, P.F., Christiansen, K.A. & Janssens, F. (1996-2019). Checklist of the
746 Collembola of the World. Available at <http://www.collembola.org>.
- 747 Bellini, B.C. and Cipola, N.G. (2017). The Neotropical genera of Paronellinae
748 (Collembola, Entomobryoidea, Paronellidae) with description of two new species
749 and redescription of *Campylothorax mitrai*. *Zootaxa* 4300(2), 151-179.
- 750 Berg, M. & Heijerman, T. (2002). De springstaart *Lepidocyrtus paradoxus* nieuw voor
751 de Nederlandse fauna (Hexapoda: Collembola). *Nederlandse Faunistische*
752 *Mededelingen*, 16, 69-75.

- 753 Bourlet, A. (1839) Mémoire sur les Podures. *Mémoires de la Société des Sciences*
754 *de l' Agriculture de Lille*, 1, 377–417.
- 755 Christiansen, K.A. and Bellinger, P.F. (1980). The Collembola of North America north
756 of Rio Grande, a taxonomic analysis. (Grinnell College, Iowa, 1518 pp).
- 757 Cicconardi, F., Fanciulli, P. P., and Emerson, B. C. (2013). Collembola, the biological
758 species concept and the underestimation of global species richness. *Molecular*
759 *Ecology* 22, 5382–5396.
- 760 Cicconardi, F., Nardi, F., Emerson, B.C., Frati, F., Fanculli, P.P. (2010). Deep
761 phylogeographic divisions and long-term persistence of forest invertebrates
762 (Hexapoda: Collembola) in the North-Western Mediterranean basin. *Molecular*
763 *Ecology* 19, 386–400.
- 764 Cipola, N.G. and Bellini, B.C. (2016). A new cave species of *Coecobrya* Yosii
765 (Collembola, Entomobryidae, Entomobryinae) from South Africa, with an
766 identification key to the genus. *Zootaxa* 4200(3), 351–366.
- 767 Cipola, N.G., de Morais J.W, and Bellini B.C. (2016a) A new genus of Entomobryinae
768 (Collembola, Entomobryidae) from Brazilian Amazon with body scales and dental
769 spines. *Zootaxa* 4105 (3): 261–273.
- 770 Cipola, N.G., de Morais, J.W. and Bellini, B.C. (2016b. A New Epigeous Species of
771 *Troglobius* (Collembola: Paronellidae: Cyphoderinae) from Brazil and Notes on the
772 Chaetotaxy of the Genus. *Florida Entomologist* 99(4), 658-666.
- 773 Cipola, N.G, de Morais J.W and Bellini B.C. (2017). The discovery of *Lepidocyrtoides*
774 Schött, 1917 (Collembola, Entomobryidae, Entomobryinae) from the New World,
775 including three new species from Brazil and one from Australia. *Zootaxa* 4324(2),
776 201–248.
- 777 Cipola, N.G, de Morais J.W and Bellini B.C. (2018a). New species, redescription
778 and a new combination of *Acanthocyrtus* Handschin, 1925 and *Amazhomidia*
779 Cipola & Bellini, 2016 (Collembola, Entomobryidae, Entomobryinae). *Zootaxa*
780 4387(3), 401–435.
- 781 Cipola, N.G, Arbea, J, Baquero, E, Jordana, R., de Morais, J.W. and Bellini, B.C.
782 (2018b). The survey of *Seira* Lubbock, 1870 (Collembola, Entomobryidae,
783 Seirinae) from Iberian Peninsula and Canary Islands, including three new species.
784 *Zootaxa* 4458 (1).
- 785 Cipola, N.G., de Morais J.W, and Bellini B.C. (2018c). New subgenus and four
786 species of *Lepidocyrtus* Bourlet (Collembola, Entomobryidae, Lepidocyrtinae) from
787 Amazon. *Insect Systematics & Evolution* 50(2), 189-234.

- 788 Cipola, N.G., de Morais J.W, Godeiro, N.N. and Bellini B.C. (2019). Taxonomic
789 revision of Brazilian genus *Tyrannoseira* Bellini & Zeppelini, 2011 (Collembola,
790 Entomobryidae, Seirinae). *Zootaxa* 4586(2), 201–248.
- 791 Deharveng, L., Jantarit, S. and Bedos, A. (2018). Revisiting *Lepidonella* Yosii
792 (Collembola: Paronellidae): character overview, checklist of world species and
793 reassessment of *Pseudoparonella doveri* Carpenter. *Annales de la Société*
794 *entomologique de France (N.S.)* 54(5), 381–400.
- 795 Ding, Y.H. and Zhang, F. (2015). Contribution to the eyed *Sinella* from China: two
796 new species and additional reports on nine known species (Collembola:
797 Entomobryidae). *Zootaxa* 3973(3), 474–490.
- 798 Fjellberg, A. (1999). The labial palp in Collembola. *Zoologischer Anzeiger*, 237, 309–
799 330.
- 800 Fjellberg, A. (2007). The Collembola of Fennoscandia and Denmark. Part II:
801 Entomobryomorpha and Symphypleona. *Fauna Entomologia Scandinavica* 42, 1–
802 264.
- 803 Gisin, H. (1944). Materialien zur Revision der Collembolen. *Bulletin de la Societe*
804 *Entomologique Suisse* 19(4/5), 121–156.
- 805 Gisin, H. (1963). Collemboles d'Europe V. *Revue Suisse de Zoologie*, 7, 77–101.
- 806 Gisin, H. (1964a). Collemboles d'Europe VI. *Revue Suisse de Zoologie*, 71(2), 383–
807 400.
- 808 Gisin, H. (1964b). Collemboles d'Europe VII. *Revue Suisse de Zoologie*, 71(4), 649–
809 678.
- 810 Gisin, H. (1967). Espèces nouvelles et lignées évolutives de *Pseudosinella* endogés
811 (Collembola). *Memórias e Estudos do Museu Zoológico da Universidade de*
812 *Coimbra* 301, 6–25.
- 813 Hall, T.A. (1999). BioEdit: a user-friendly biological sequence alignment editor and
814 analysis program for Windows 95/98/NT. *Nucleic Acids Symposium Ser.* 41, 95–
815 98.
- 816 Hopkin, S.P. (1997). *Biology of the Springtails (Insecta: Collembola)*. (Oxford
817 University Press, Oxford, 330 pp).
- 818 Hopkin, S.P. (2007). *A Key to the Collembola (springtails) of Britain and Ireland*.
819 (Field Studies Council, 252 pp).
- 820 Hüther, W. (1986) New aspects in taxonomy of *Lepidocyrtus* (Collembola). In '2nd
821 International Seminar on Apterygota' (Ed R.Dallai) pp. 61–65.

- 822 Jantarit, S., Satasook, Ch and Deharveng, L. (2014). *Cyphoderus* (Cyphoderidae) as
823 a major component of collembolan cave fauna in Thailand, with description of two
824 new species. *ZooKeys* 368,1–21.
- 825 Jantarit, S., Satasook, Ch. and Deharveng, L. (2019). *Coecobrya sirindhornae* sp. n.,
826 the most highly troglomorphic Collembola in Southeast Asia (Collembola,
827 Entomobryidae). *Zookeys* 824, 21-44.
- 828 Katoh, K., Rozewicki, J., Yamada, K.D. (2019). MAFFT online service: Multiple
829 sequence alignment, interactive sequence choice and visualization. *Brief*
830 *Bioinform* 20, 1160–1166.
- 831 Katz, A. D., Giordano, R., and Soto-Adames, F. (2015). Taxonomic review and
832 phylogenetic analysis of fifteen North American *Entomobrya* (Collembola,
833 Entomobryidae), including four new species. *ZooKeys* 525, 1–75.
- 834 Lanfear, R., Frandsen, P.B., Wright, A.M., Senfeld, T., Calcott, B. (2017).
835 Partitionfinder 2: New methods for selecting partitioned models of evolution for
836 molecular and morphological phylogenetic analyses. *Molecular Biology and*
837 *Evolution* 34, 772–773.
- 838 Letunic, I. and Bork, P. (2019). Interactive Tree Of Life (iTOL) v4: recent updates and
839 new developments. *Nucleic Acids Research* 47, 256–259.
- 840 Lubbock, J. (1873). 'Monograph of the Collembola and Thysanura'. (The Ray
841 Society, London, 276 pp).
- 842 Lukić, M., Delić, T., Zagmajster, M., and Deharveng, L. (2018). Setting a
843 morphological framework for the genus *Verhoeffiella* (Collembola, Entomobryidae)
844 for describing new troglomorphic species from the Dinaric karst (Western
845 Balkans). *Invertebrate Systematics* 32(5), 1118–1170.
- 846 Lukić, M., Porco, D., Bedos, A. and Deharveng, L. (2015). The puzzling distribution of
847 *Heteromurus* (*Verhoeffiella*) *absoloni* Kseneman, 1938 (Collembola:
848 Entomobryidae: Heteromurinae) resolved: detailed redescription of the nominal
849 species and description of a new species from Catalonia (Spain). *Zootaxa*
850 4039(2), 249–275.
- 851 Ma, Y. and Shi, S. (2018). Three new species of *Entomobrya* (Collembola:
852 Entomobryidae) from China. *European Journal of Taxonomy* 419, 1–21.
- 853 Mari Mutt, J.A. (1986) Puerto Rican species of *Lepidocyrtus* and *Pseudosinella*
854 (Collembola: Entomobryidae). *Caribbean Journal of Sciences* 22(1–2), 1–48.
- 855 Mateos, E. (2008a). The European *Lepidocyrtus* Bourlet, 1839 (Collembola:
856 Entomobryidae). *Zootaxa* 1769, 35–59.

- 857 Mateos, E. (2008b). Definition of *Lepidocyrtus lusitanicus* Gama, 1964 species-
858 complex (Collembola, Entomobryidae), with description of new species and color
859 forms from the Iberian Peninsula. *Zootaxa* 1917, 38–54.
- 860 Mateos, E. (2011). New *Lepidocyrtus* Bourlet, 1839 taxa from Greece (Collembola:
861 Entomobryidae). *Zootaxa* 3108, 25–40.
- 862 Mateos, E. (2012). The European *Lepidocyrtus lanuginosus* group (Collembola:
863 Entomobryidae), definition and description of a new species from Spain. *Zootaxa*
864 3570, 69–81.
- 865 Mateos, E. and Winkler, D. (2018). New data clarifying the taxonomy of European
866 members of the *Lepidocyrtus pallidus* - *serbicus* group (Collembola,
867 Entomobryidae). *Zootaxa* 4429 (3), 548-568.
- 868 Mateos, E., and Greenslade, P. (2015). Towards understanding *Lepidocyrtus*
869 Bourlet, 1839 (Collembola, Entomobryidae) I: diagnosis of the subgenus
870 *Setogaster*, new records and redescriptions of species. *Zootaxa* 4044(1), 105–
871 129.
- 872 Mateos, E., and Petersen, H. (2012). Definition of the European *Lepidocyrtus*
873 *curvicollis* group (Collembola: Entomobryidae) with description of a new species
874 from Sardinia (Italy). *Zootaxa* 3273, 51–62.
- 875 Mateos, E., Escuer, P., Busmachiu, G., Riutort, M., and Álvarez-Presas, M. (2018).
876 Untangling *Lepidocyrtus* (Collembola, Entomobryidae): new molecular data shed
877 light on the relationships of the European groups. *Invertebrate Systematics* 32,
878 639–651.
- 879 Miller, M.A., Pfeiffer, W. and Schwartz, T. (2010). Creating the CIPRES Science
880 Gateway for Inference of Large Phylogenetic Trees, in 'Proceedings of the
881 Gateway Computing Environments Workshop (GCE)'. pp. 1–8 (New Orleans, LA).
- 882 Minh, B.Q., Nguyen, M.A.T. and Von Haeseler, A. (2013). Ultrafast approximation for
883 phylogenetic bootstrap. *Molecular Biology and Evolution* 30, 1188–1195.
- 884 Nguyen, L.T., Schmidt, H.A., Von Haeseler, A. and Minh, B.Q. (2015). IQ-TREE: A
885 fast and effective stochastic algorithm for estimating maximum-likelihood
886 phylogenies. *Molecular Biology and Evolution* 32, 268–274.
- 887 Nilsai, A., Jantarit, S., Satasook, C., and Zhang, F. (2017). Three new species of
888 *Coecobrya* (Collembola: Entomobryidae) from caves in the Thai peninsula.
889 *Zootaxa* 4286, 187–202.
- 890 Nunes, R.D. and Bellini, B.C. (2018). Three new species of Entomobryoidea
891 (Collembola: Entomobryomorpha) from Brazilian Caatinga-Cerrado transition, with

- 892 identification keys to Brazilian *Cyphoderus*, *Pseudosinella* and *Trogolaphysa*
893 species. *Zootaxa* 4420 (1): 071–096.
- 894 Pan, Z.X., Zhang, F. and Li, Y.B. (2015). Two closely related *Homidia* species
895 (Entomobryidae, Collembola) revealed by morphological and molecular evidence.
896 *Zootaxa* 3918 (2): 285–294.
- 897 Parfitt, E. (1891). Devon Collembola and Thysanura. *Transactions of the Devonshire*
898 *Association for the Advancement of Science Literature and Art*, 23, 322–352.
- 899 Puillandre, N., Lambert, A., Brouillet, S. and Achaz, G. (2012). ABGD, Automatic
900 Barcode Gap Discovery for primary species delimitation. *Molecular Ecology* 21,
901 1864–1877.
- 902 Rambaut, A. (2009). 'FigTree. Tree figure drawing tool'. Available at
903 <http://tree.bio.ed.ac.uk/software/figtree/>.
- 904 Ren, Y., Li, Z. and Zhang, F. (2018). A new species of *Dicranocentrus* Schött from
905 Hainan (China) with a key to the Chinese species of the genus (Collembola,
906 Entomobryidae). *ZooKeys* 762, 59–68.
- 907 Ronquist, F., Teslenko, M., van der Mark, P., Ayres, D.L., Darling, A., Höhna, S.,
908 Larget, B., Liu, L., Suchard, M.A. and Huelsenbeck, J.P. (2012). MrBayes 3.2:
909 Efficient Bayesian Phylogenetic Inference and Model Choice Across a Large
910 Model Space. *Systematics Biology* 61, 539–542.
- 911 Santos, I.P.S., Cipola, N.G., de Moraes, J.W. and Bellini, B.C. (2016). A new species
912 of *Campylothorax* (Collembola: Paronellidae: Paronellinae) from Northern Brazil.
913 *Zoologia* 33(3), 1–6.
- 914 Snider, R.J. (1967). The chaetotaxy of North American *Lepidocyrtus* s. str.,
915 (Collembola: Entomobryidae). *Contributions of the American Entomological*
916 *Institute* 2(3), 1–28.
- 917 Soto-Adames, F. N. (2010). Two new species and descriptive notes for five
918 *Pseudosinella* species (Hexapoda: Collembola: Entomobryidae) from West
919 Virginian (USA) caves. *Zootaxa* 2331, 1–34.
- 920 Szeptycki, A. (1967). Morpho-systematic studies on Collembola. Part 1. Materials to
921 a revision of the genus *Lepidocyrtus* Bourlet, 1839 (Entomobryidae s.l.). *Acta*
922 *Zoologica Cracoviensa* 12(13), 369–377.
- 923 Szeptycki, A. (1972). Morpho-systematic studies on Collembola III. Body chaetotaxy
924 in the first instars of several genera of the Entomobryomorpha. *Acta Zoologica*
925 *Cracoviensia* 17, 341–372.

- 926 Szeptycki, A. (1979) Chaetotaxy of the Entomobryidae and its phylogenetical
927 significance. Morpho-systematic studies of Collembola, IV. Polska Akademia
928 Nauk, Zakład Zoologii Systematycznej i Doświadczalnej, Kraków, Poland, 219 pp.
- 929 Talavera, G. and Castresana, J. (2007). Improvement of Phylogenies after Removing
930 Divergent and Ambiguously Aligned Blocks from Protein Sequence Alignments.
931 *Systematic Biology* 56(4), 564–577.
- 932 Wang, F., Chen, J.X. and Christiansen, K. (2003). Taxonomy of the genus
933 *Lepidocyrtus* s.l. (Collembola: Entomobryidae) in East and Southeast Asia and
934 Malaysia, with description of a new species from the People's Republic of China.
935 *Canadian Entomologist* 135, 823–837.
- 936 Winkler, D. (2016). A new species of *Lepidocyrtus* (Collembola, Entomobryidae) from
937 the Börzsöny Mountains, Hungary. *Zootaxa* 4150(4): 388–400.
- 938 Winkler, D. (2017). New *Lepidocyrtus* Bourlet, 1839 from riverine woodland in
939 Hungary (Collembola, Entomobryidae). *Zootaxa* 4250(6), 529–540.
- 940 Winkler, D. and Mateos, E. (2018). Redescription of *Lepidocyrtus peisonis* Traser &
941 Christian, 1992 with notes on *Lepidocyrtus mariani* Traser & Dányi, 2008
942 (Collembola: Entomobryidae). *Zootaxa* 4375 (3): 392–408.
- 943 Winkler, D., and Traser, G. N. (2012). Explanation of the European *Lepidocyrtus*
944 *pallidus-serbicus* group (Collembola, Entomobryidae), with description of new
945 species from Hungary. *Zootaxa* 3394, 35–47.
- 946 Yu, D., Zhang, F. and Deharveng, L. (2014). A peculiar cave species of *Tomocerus*
947 (Collembola, Tomoceridae, Tomocerinae) from Vietnam, with a discussion of the
948 postantennal organ and prelabral chaetae in Tomocerinae. *ZooKeys* 408: 61–70.
- 949 Zhang, B., Chen, T. W., Mateos, E., Scheu, S., and Schaefer, I. (2018a). Cryptic
950 species in *Lepidocyrtus lanuginosus* (Collembola: Entomobryidae) are sorted by
951 habitat type. *Pedobiologia* 68, 12–19.
- 952 Zhang, B., Chen, T. W., Mateos, E., Scheu, S., and Schaefer, I. (2019a). DNA-based
953 approaches uncover cryptic diversity in the European *Lepidocyrtus lanuginosus*
954 species group (Collembola: Entomobryidae). *Invertebrate Systematics* 2019(33),
955 661–670.
- 956 Zhang, F., Bellini, B.C. and Soto-Adames, F.N. (2019b). New insights into the
957 systematics of Entomobryoidea (Collembola: Entomobryomorpha): first instar
958 chaetotaxy, homology and classification. *Zoological Systematics* 44(4), 249–278.
- 959 Zhang, F. and Dong, R.R. (2014). Three new species of *Coecobrya* (Collembola:
960 Entomobryidae) from southern and northwest China. *Zootaxa* 3760(2), 260–274.

- 961 Zhang, F., Jantarit, S., Nilsai, A., Stevens, M. I., Ding, Y., and Satasook, C. (2018b).
962 Species delimitation in the morphologically conserved *Coecobrya* (Collembola:
963 Entomobryidae): a case study integrating morphology and molecular traits to
964 advance current taxonomy. *Zoologica Scripta* 47, 342–356.
965

For Review Only

966 **Tables**

967

968 Table 1. Localities of the studied species. Abb: abbreviations of species names used
969 on other sections of the manuscript. * species studied only morphologically.

970

971 Table 2. List of sequences used for the molecular phylogenetic inferences and the
972 molecular species delimitation analyses with GenBank Accession numbers.

973

974 Table 3. Number of pseudopores on each position for all species studied. For each
975 position the pseudopores number on one side of the body is indicated, except
976 numbers between parentheses which correspond to odd groups of pseudopores
977 located at the centre of the segments involved. Pos, position number. lu, lusitanicus-
978 group; la, lanuginosus-group; pa, pallidus–serbicus-group; li, lignorum-group; cu,
979 curvicollis-group. *, same pseudopores number for all species in this position. #1,
980 including species: bic+cya+lan. #2, including species: cho+lig1+pul+spJ+spK+tra.
981 See Table 1 for explanation of abbreviations used for each species.

982

983 Table 4. *Lepidocyrtus violaceus*. Number of pseudopores on each position for each
984 population studied. Pos, position number. #: including populations A1 + A3 + B1 +
985 B2 + B3 + C + D + F1 + F2. See **Table 1** for explanation of abbreviations used for
986 each species.

987

988 Table 5. *Lepidocyrtus violaceus*. Differential characters between populations. ABGD,
989 molecular entities detected by the ABGD delimitation analysis. N, number of
990 specimens morphologically studied. Size, body size (without head) in mm. Ocular-q,
991 presence or absence of interocular chaeta q. Abd.II-ml, presence or absence of
992 chaeta ml on Abd.II. Abd.II-p5p, presence or absence of chaeta p5p on Abd.II.
993 Abd.III-mi, presence or absence of chaeta mi on Abd.III. Abd.III-d3, presence or
994 absence of chaeta d3 on Abd.III. B4-B5/B5-B6, ratio between distances of
995 macrochaetae B4 to B5 and B5 to B6 on Abd.IV. Abd.IV-B6, shape of macrochaeta
996 B6 on Abd.IV, bcm = broad ciliated macrochaeta, tcm = thin ciliated
997 macrochaeta. BP4-pse, presence (+) or absence (-) of pseudopores on BP4. In all
998 cases: +=present, -=absent, -/+ =absent or present depending on the specimen, (-
999 /+)=absent or present as intraindividual asymmetry.

1000

1001 **Figures**

1002

1003 Figure 1. Tree inferred with the Concatenated dataset using Bayesian Inference.
1004 Numbers at nodes correspond to Posterior Probability (PP) over the branch and
1005 bootstrap values obtained in the ML inference, under the branch. Clade “*lignorum*
1006 group” is detailed in **Figure 2**. Tree scale indicates number of substitutions per site.
1007 Outgroups correspond to the genera *Orchesella* and *Cyphoderus* gr. *bidenticulati*. To
1008 the right of the tree, the color bars and associated labels indicate the molecular
1009 entities inferred with the ABGD species delimitation analysis.

1010

1011 Figure 2. Clade “*lignorum* group”. Tree inferred with the Concatenated dataset using
1012 Bayesian Inference. Numbers at nodes correspond to Posterior Probability (PP) over
1013 the branch and bootstrap values obtained in the ML inference, under the branch.
1014 Tree scale indicates number of substitutions per site. To the right of the tree, the
1015 color bars and associated labels indicate the molecular entities inferred with the
1016 ABGD species delimitation analysis. The pictures show the habitus of the different
1017 molecular entities of *Lepidocyrtus violaceus* predicted with the ABGD analysis.

1018

1019 Figure 3. *Lepidocyrtus violaceus*. Map of Europe showing the localities (black dots)
1020 where specimens were collected. See Table 1 for the explanation of LP#### sample
1021 codes.

1022

1023 Figure 4. *Lepidocyrtus* sp. Dorsal view of the head. Black arrows point to
1024 pseudopores (black dots) on positions 4 and 5.

1025

1026 Figure 5. *Lepidocyrtus* sp. Basal portion of the anterior region of manubrium and
1027 ventral region of abdominal segments V – VI. (a) female, (b) male. The two superior
1028 arrows point to pseudopores located on manubrium (position 13). The inferior arrow
1029 points to a pseudopore located on Abd.V in front of the genital plate (position 27).

1030

1031 Figure 6. *Lepidocyrtus* sp. Apex of ventral region of second antennal joint. The white
1032 arrow points to a pseudopore on position 17.

1033

1034 Figure 7. *Lepidocyrtus* sp. Ventral view of abdominal segments I – III. Pseudopores
1035 on positions 23 and 24 are inside the white circles.

1036

1037 Figure 8. *Lepidocyrtus* sp. Ventral view of the third abdominal segment showing the
1038 retinaculum. The white arrows point to pseudopores on position 25.

1039

1040 Figure 9. *Lepidocyrtus* sp. Distribution of pseudopores on dorsal positions. Black dots
1041 are pseudopores common to all species. Arrows point to dorsal positions where
1042 pseudopores vary between species-groups *lusitanicus* (lu), *lanuginosus* (la), *pallidus*
1043 (pa), *lignorum* (li) and *curvicollis* (cu). Under each species-group abbreviation the
1044 number of pseudopores on each position is indicated.

1045

1046 Figure 10. *Lepidocyrtus* sp. Distribution of pseudopores on ventral+lateral positions.
1047 Black dots are pseudopores common to all species. Arrows point to ventral and
1048 lateral positions where pseudopores vary between species-groups *lusitanicus* (lu),
1049 *lanuginosus* (la), *pallidus* (pa), *lignorum* (li) and *curvicollis* (cu). Under each species-
1050 group abbreviation the number of pseudopores on each position is indicated.

1051

1052 Figure 11. *Lepidocyrtus* sp. lateral habitus. Shaded areas are the positions where
1053 pseudopores can be located on Abd.IV. Numbers refer to positions (see [Table 3](#)).
1054 Dashed arrow indicates that position 26 is located on the ventral region of the
1055 segment.

1056

1057 Figure 12. *Lepidocyrtus violaceus*. Distribution of pseudopores (black dots) on dorsal
1058 (left image) and ventral+lateral positions.

1059

1060 Figure 13. *Lepidocyrtus violaceus*. Right ocular area. A – G eyes. The arrow points to
1061 chaeta q, that is present or absent depending on the specimens.

1062

1063 Figure 14. *Lepidocyrtus violaceus*. Dorsal scheme of (a) Abd.II and (b) Abd. III
1064 chaetotaxy (left side). Arrows point to chaetae that are present or absent depending
1065 on the specimens.

1066

1067 Figure 15. *Lepidocyrtus violaceus*. Dorsal scheme of abd.IV chaetotaxy (left side).
1068 Dashed rectangle delimits chaetae B4, B5 and B6 on specimens with ratio $B4-B5/B5-$
1069 $B6 < 2$ (a) and ratio $B4-B5/B5-B6 > 2$ (b). Large black dots indicate broad ciliated
1070 macrochaetae, small black dots indicate thin ciliated macrochaetae.

Table 1.

Sample code	Genus	Species	Abb	Municipality	Province/County	Country	Position (WGS84)	Collecting date
LP325	<i>Lepidocyrtus</i>	<i>arrabonicus</i>	arr	Morasti	Braşov	Romania	N45.2245 E24.5019	01.iv.2013
LP239	<i>Lepidocyrtus</i>	<i>barbulus</i>	bar	Kakopetros	Creta	Greece	N35.408150 E23.755342	07.iv.2009
LP190	<i>Lepidocyrtus</i>	<i>bicoloris</i>	bic	Cabrils	Barcelona	Spain	N41.54661 E2.36532	28.xi.2007
LP175	<i>Lepidocyrtus</i>	<i>bilobatus</i>	bil	Sotoserrano	Salamanca	Spain	N40.4110 W6.0535	02.viii.2007
LP383	<i>Lepidocyrtus</i>	<i>chorus</i>	cho	Sibenick	Miljacka	Croatia	N44.001145 E16.018398	29.iv.2015
*LP580	<i>Lepidocyrtus</i>	<i>curvicollis</i>	cur	St Laurent de Minier	Gard	France	N43.93823 E3.67255	30.vii.1991
LP277	<i>Lepidocyrtus</i>	<i>cyaneus</i>	cya	Torla	Huesca	Spain	N42.6840719 W0.1118863	31.v.2009
LP223	<i>Lepidocyrtus</i>	<i>flexicollis</i>	fle	Alcalá de los Gazules	Cádiz	Spain	N36.5222285 W5.6501549	28.ii.2009
LP114	<i>Lepidocyrtus</i>	<i>intermedius</i>	int	Aiguafreda	Barcelona	Spain	N41.7999 E2.3007	10.ii.2007
LP229	<i>Lepidocyrtus</i>	<i>juliae</i>	jul	Georgioupoli	Creta	Greece	N35.360540 E24.251808	07.iv.2009
LP130	<i>Lepidocyrtus</i>	<i>lanuginosus</i>	lan	Vallgorguina	Barcelona	Spain	N41.6583 E2.5199	18.iv.2007
LP118	<i>Lepidocyrtus</i>	<i>lignorum</i>	lig1	Barcelona	Barcelona	Spain	N41.448950 E2.140780	18.ii.2007
LP266	<i>Lepidocyrtus</i>	<i>lignorum</i>	lig2	Drios	Paros	Greece	N37.000678 E25.197013	10.iv.2009
LP100	<i>Lepidocyrtus</i>	<i>lusitanicus</i>	lus	Poblet	Tarragona	Spain	N41.35677 E1.07869	03.i.2007
*LP455	<i>Lepidocyrtus</i>	<i>mariani</i>	mar	Nagykapornak	Zala	Hungary	N46°50'35" E16°58'26"	15.vii.2015
LP129	<i>Lepidocyrtus</i>	<i>montseniensis</i>	mon	Vallgorguina	Barcelona	Spain	N41.6583 E2.5199	18.iv.2007
LP362	<i>Lepidocyrtus</i>	<i>pallidus</i>	pal	Tjôme	Vestfold	Norway	N59.1521 E10.4321	06.iv.2014
LP328	<i>Lepidocyrtus</i>	<i>paradoxus</i>	par	Chisinau	Moldova	Moldova	N47.0354 E28.7981	20.iii.2013
LP389	<i>Lepidocyrtus</i>	<i>pulchellus</i>	pul	Varese Ligure	La Spezia	Italy	44°22'48.53"N, 9°30'40.63"E	04.v.2015
LP195	<i>Lepidocyrtus</i>	<i>selvaticus</i>	sel	Tossa de Mar	Girona	Spain	N41.71908 E2.90280	21.ii.2008
LP234	<i>Lepidocyrtus</i>	<i>serbicus</i>	ser	Kalamafka	Creta	Greece	N35.080339 E25.650831	06.iv.2009
LP125	<i>Lepidocyrtus</i>	<i>spJ</i>	spj	Sant Celoni	Barcelona	Spain	N41.66449 E2.56279	18.iv.2007
LP108	<i>Lepidocyrtus</i>	<i>spK</i>	spk	Aiguafreda	Barcelona	Spain	N41.7892 E2.3113	10.ii.2007
LP122	<i>Lepidocyrtus</i>	<i>spK</i>	spk	Sinarcas	Valencia	Spain	N39.765328 W1.226981	02.iv.2007
LP250	<i>Lepidocyrtus</i>	<i>spL</i>	spl	Laerma	Rodas	Greece	N36.146639 E27.920374	04.iv.2009

LP106	<i>Lepidocyrtus</i>	<i>tellecheae</i>	tel	Aiguafreda	Barcelona	Spain	N41.7705 E2.2722	10.ii.2007
LP546	<i>Lepidocyrtus</i>	<i>traseri</i>	tra	Nagybörzsöny	Pest	Hungary	N 47°53'54" E18°51'10"	05.10.2017
LP061	<i>Lepidocyrtus</i>	<i>violaceus</i>	vio	Huesca	Huesca	Spain	N42.599770 E0.756810	19.vii.2006
LP065	<i>Lepidocyrtus</i>	<i>violaceus</i>	vio	Vall d'Aran	Lleida	Spain	N42.777980 E0.834220	19.vii.2006
LP068	<i>Lepidocyrtus</i>	<i>violaceus</i>	vio	Caldes de Boi	Lleida	Spain	N42.553490 E0.832250	20.vii.2006
LP076	<i>Lepidocyrtus</i>	<i>violaceus</i>	vio	Vall d'Aran	Lleida	Spain	N42.628210 E0.762160	20.vii.2006
LP096	<i>Lepidocyrtus</i>	<i>violaceus</i>	vio	Pontedeume	A Coruña	Spain	N43.417185 W8.063563	11.xi.2006
LP101	<i>Lepidocyrtus</i>	<i>violaceus</i>	vio	Cogullons	Tarragona	Spain	N41.334020 E1.077590	03.i.2007
LP157	<i>Lepidocyrtus</i>	<i>violaceus</i>	vio	Gerês	Braga	Portugal	N41.7507 W8.1528	14.vii.2007
LP159	<i>Lepidocyrtus</i>	<i>violaceus</i>	vio	Coimbra	Coimbra	Portugal	N40.2092 W8.4191	19.vii./2007
LP392	<i>Lepidocyrtus</i>	<i>violaceus</i>	vio	Bugeac	Gagaucia	Moldova	N46.36606 E28.6757	20.iv.2013
LP457	<i>Lepidocyrtus</i>	<i>violaceus</i>	vio	Villaggio San Michelle	Trentino-Alto Adigio	Italy	45°42'15.73"N, 10°58'23.94"E	04.v.2015
LP539	<i>Lepidocyrtus</i>	<i>violaceus</i>	vio	Poblet	Tarragona	Spain	N41.35677 E1.07869	28.xii.2017
LP543	<i>Lepidocyrtus</i>	<i>violaceus</i>	vio	Csáfordjánosfa	Győr-Moson-Sopron	Hungary	N 47°24'45" E 16°57'52"	15.iv.2017
LP544	<i>Lepidocyrtus</i>	<i>violaceus</i>	vio	Nagymaros	Pest	Hungary	N 47°46'34" E18°55'42"	11.iv.2017
LP545	<i>Lepidocyrtus</i>	<i>violaceus</i>	vio	Sopron	Győr-Moson-Sopron	Hungary	N 47°40'39" E16°27'35"	10.xi.2018
LP440	<i>Cyphoderus</i>	<i>gr.bidenticulati</i>	Cyp	Cellers	Lleida	Spain	N42°03'41.4" E0°54'04.7"	01.xii.2015
Orches	<i>Orchsella</i>	<i>sp</i>	–	–	–	–	–	–

Table 2.

<i>Species</i>	Code	GenBank Accession Number	
		COII	EF-1 α
<i>Lepidocyrtus arrabonicus</i>	LP325_1	MF095510	-
	LP325_3	MF095512	MF095603
<i>Lepidocyrtus barbulus</i>	LP239_1	MF095498	MF095594
	LP239_2	MF095499	MF095595
<i>Lepidocyrtus bicoloris</i>	LP190_3	MF095482	MF095584
	LP190_4	MF095483	MF095585
<i>Lepidocyrtus bilobatus</i>	LP175_1	MF095533	-
	LP175_2	MF095532	MF095615
<i>Lepidocyrtus chorus</i>	LP383_1	MF095522	MF095609
	LP383_2	MF095523	-
<i>Lepidocyrtus cyaneus</i>	LP277_1	MF095506	MF095600
	LP277_2	MF095507	MF095601
<i>Lepidocyrtus flexicolis</i>	LP223_1	MF095485	MF095587
	LP223_2	MF095486	MF095588
<i>Lepidocyrtus intermedius</i>	LP114_1	MF095458	-
	LP114_2	MF095459	MF095569
<i>Lepidocyrtus juliae</i>	LP229_1	MF095490	MF095590
	LP229_2	MF095491	-
<i>Lepidocyrtus lanuginosus</i>	LP130_1	MF095474	MF095579
	LP130_2	MF095475	MF095574
<i>Lepidocyrtus lignorum</i>	LP118_1	MF095465	MF095570
	LP118_2	MF095466	*
	LP266_1	MF095503	MF095597
<i>Lepidocyrtus lusitanicus</i>	LP100_1	MF095537	MF095614
	LP100_2	MF095540	-
<i>Lepidocyrtus montseniensis</i>	LP129_1	MF095470	MF095571
	LP129_2	MF095471	MF095572
<i>Lepidocyrtus pallidus</i>	LP362_3	MF095519	MF095608
	LP362_4	MF095520	-
<i>Lepidocyrtus paradoxus</i>	LP328_1	MF095514	MF095605
	LP328_2	MF095515	MF095606
<i>Lepidocyrtus pulchellus</i>	LP389_7	*	-
	LP389_8	*	*
<i>Lepidocyrtus selvaticus</i>	LP195_1	MF095542	MF095616
	LP195_2	MF095544	-
<i>Lepidocyrtus serbicus</i>	LP234_3	MF095495	MF095591
	LP234_4	MF095496	MF095592
<i>Lepidocyrtus tellecheae</i>	LP106_2	MF095529	MF095564
	LP106_3	MF095530	MF095565
<i>Lepidocyrtus traseri</i>	LP546_1	*	*
	LP546_2	*	*
	LP546_3	*	*
<i>Lepidocyrtus violaceus</i>	LP061_1	*	*
	LP061_2	*	*
	LP061_3	*	*
	LP061_4	*	*
	LP061_5	*	*
	LP065_1	MF095436	MF095558

LP065_2	*	*
LP068_1	*	-
LP068_2	*	*
LP068_3	*	*
LP068_4	*	*
LP076_4	*	-
LP076_5	*	*
LP076_6	*	-
LP076_7	*	*
LP096_1	*	*
LP096_2	*	*
LP096_3	*	*
LP096_4	*	*
LP096_5	*	*
LP101_3	*	-
LP101_4	*	*
LP157_1	*	*
LP157_2	*	*
LP157_3	*	*
LP157_4	*	*
LP157_5	*	*
LP159_1	*	*
LP159_2	*	*
LP159_3	*	*
LP159_4	*	*
LP392_2	*	-
LP457_4	*	*
LP457_5	*	*
LP539_5	*	*
LP539_6	*	*
LP539_7	*	-
LP539_8	*	*
LP543_1	*	*
LP543_3	*	*
LP544_1	*	*
LP544_2	*	*
LP544_3	*	*
LP545_1	*	*
LP545_2	*	*
LP545_3	*	*
<i>Lepidocyrtus spJ</i>		
LP125_1	*	*
LP125_2	*	*
LP125_3	*	*
LP125_4	*	*
LP125_5	*	*
<i>Lepidocyrtus spK</i>		
LP108_1	*	*
LP108_2	*	*
LP108_3	*	*
LP108_4	*	*
LP108_5	*	*
LP122_1	*	*

	LP122_2	*	*
	LP122_3	*	*
	LP122_4	*	*
	LP122_5	*	*
<i>Lepidocyrtus spL</i>	LP250_4	*	-
	LP250_5	*	*
	LP250_6	*	-
	LP250_7	*	-
OUTGROUP			
<i>Orchesella sp.</i>	Orches	EU016195	AY305473
<i>Cyphoderus gr bidenticulati</i>	LP440_1	MF095526	MF095612
	LP440_2	MF095527	MF095613

For Review Only

Table 3.

Body region	Position	Pos	lu bil+lus	lu sel	la #1	pa arr+pal	pa ser	li bar	li #2	li int	li jul	li lig2	li spL	li tel	li vio	cu cur	cu fle	cu mar	cu mon	cu par	Cyp	
Legs	Cx.I	1	2	1	2	2	2	2	2	2	2	2	2	2	2	2	2	2	2	2	2	
	Cx.II	2	2	2	2	2	2	3-5 ^a	4	2	3	3	4	6	4	5	4	5-8 ^a	3	4	2	
	*Cx.III	3	2	2	2	2	2	2	2	2	2	2	2	2	2	2	2	2	2	2	2	
Head dorsal	*Cephalic - exterior	4	1	1	1	1	1	1	1	1	1	1	1	1	1	1	1	1	1	1	1	
	*Cephalic - interior	5	2	2	2	2	2	2	2	2	2	2	2	2	2	2	2	2	2	2	1-2	
Body dorsal	*Th.II (mid dorsal)	6	1	1	1	1	1	1	1	1	1	1	1	1	1	1	1	1	1	1	1	
	*Th.III (mid dorsal)	7	1	1	1	1	1	1	1	1	1	1	1	1	1	1	1	1	1	1	1	
	*Abd.I (mid dorsal)	8	1	1	1	1	1	1	1	1	1	1	1	1	1	1	1	1	1	1	1	
	*Abd.II (mid dorsal)	9	1	1	1	1	1	1	1	1	1	1	1	1	1	1	1	1	1	1	1	
	*Abd.III (mid dorsal)	10	1	1	1	1	1	1	1	1	1	1	1	1	1	1	1	1	1	1	1	
	*Abd.IV (mid dorsal)	11	1	1	1	1	1	1	1	1	1	1	1	1	1	1	1	1	1	1	1	1
	Abd.IV (dorsal)	12	-	-	-	-	-	-	-	-	-	-	-	-	-	5-7	-	-	-	-	-	3 ^c
Furca dorsal	*Manubrial base	13	2	2	2	2	2	2	2	2	2	2	2	2	2	?	2	2	2	2	-	
	Manubrial plate	14	2	2	2	2	2	2	2	2	2	2	2	2	2	?	2	3	2	2	2	
	Dentes	15	-	-	-	1	1	2-4 ^a	2	2	1	1	2	3	2	11	3-5	11-17 ^a	2	5	-	
Antenna ventral	Ant.III	16	1	1	1	1	1	1	1	1	1	1	1	1	3	1	5	1	1	1	1	
	Ant.II	17	-	-	-	1	1	1	1	1	1	1	1	1	4	2	7	1-2	3	1	1	
	Ant.I	18	-	-	-	-	-	-	-	-	-	-	-	-	2	1	5	1-2	2	-	-	
Body ventral	*Th.I	19	1	1	1	1	1	1	1	1	1	1	1	1	1	1	1	1	1	1	1	
	*Th.II	20	1	1	1	1	1	1	1	1	1	1	1	1	1	1	1	1	1	1	1	
	*Th.III	21	1	1	1	1	1	1	1	1	1	1	1	1	1	1	1	1	1	1	1	
	*Abd.I - VT base anterior	22	1	1	1	1	1	1	1	1	1	1	1	1	1	1	1	1	1	1	1	
	*Abd.I - VT base posterior	23	1	1	1	1	1	1	1	1	1	1	1	1	1	¿	1	1	1	1	1	
	Abd.II	24	(3)	(3)	(2)	(3)	(3-5)	(5)	(3)	(3)	(3)	(3)	(3)	(3)	(3-4)	(?)	(3)	(3)	(3-4)	(3)	(4)	
	*Abd.III - post ret	25	(2)	(2)	(2)	(2)	(2)	(2)	(2)	(2)	(2)	(2)	(2)	(2)	(2)	(2)	(2)	(2)	(2)	(2)	(2)	
	Abd.IV	26	-	-	-	-	-	-	-	-	-	-	-	-	-	6-10 ^a	8	2	-	-	-	
*Abd.V – pre genital plate	27	(1)	(1)	(1)	(1)	(1)	(1)	(1)	(1)	(1)	(1)	(1)	(1)	(1)	(1)	(1)	(1)	(1)	(1)	(1)		
Body lateral	Th.III	28	-	-	-	-	-	-	-	-	-	-	-	-	-	-	-	5	-	-	-	
	Abd.I	29	-	-	-	-	-	-	-	-	-	-	-	-	-	-	-	13	-	-	-	
	Abd.II	30	-	-	-	-	-	-	-	-	-	-	-	-	-	-	-	8	-	-	-	
	Abd.III	31	-	-	-	-	-	-	-	-	-	-	-	-	-	-	-	8	-	-	-	
	Abd.IV	32	-	-	-	-	-	-	-	-	-	-	-	-	-	-	-	34	-	-	-	
	BP4	33	-	-	-	-	-	-	-	-	10	6	6	-	0-7 ^b	-	-	-	-	-	-	

^a the number of pseudopores on this position depends on the specimen size.

^bonly one population of morphological species *L. violaceus* has pseudopores on this position.

^c in *Cyphoderus* these pseudopores are not on position 12 but on the basal part of dorsal Abd.IV.

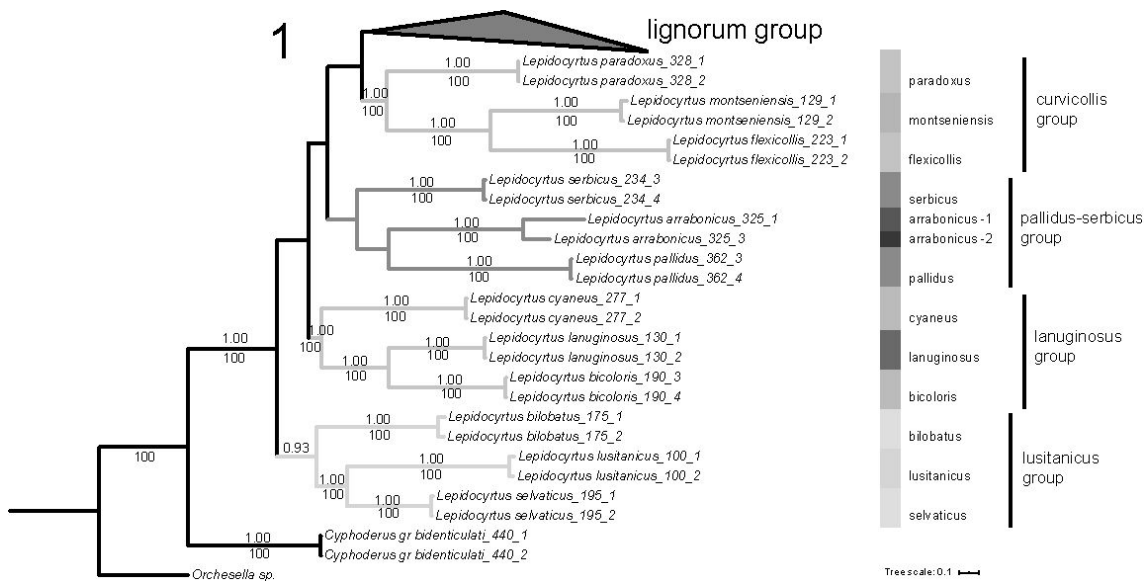
For Review Only

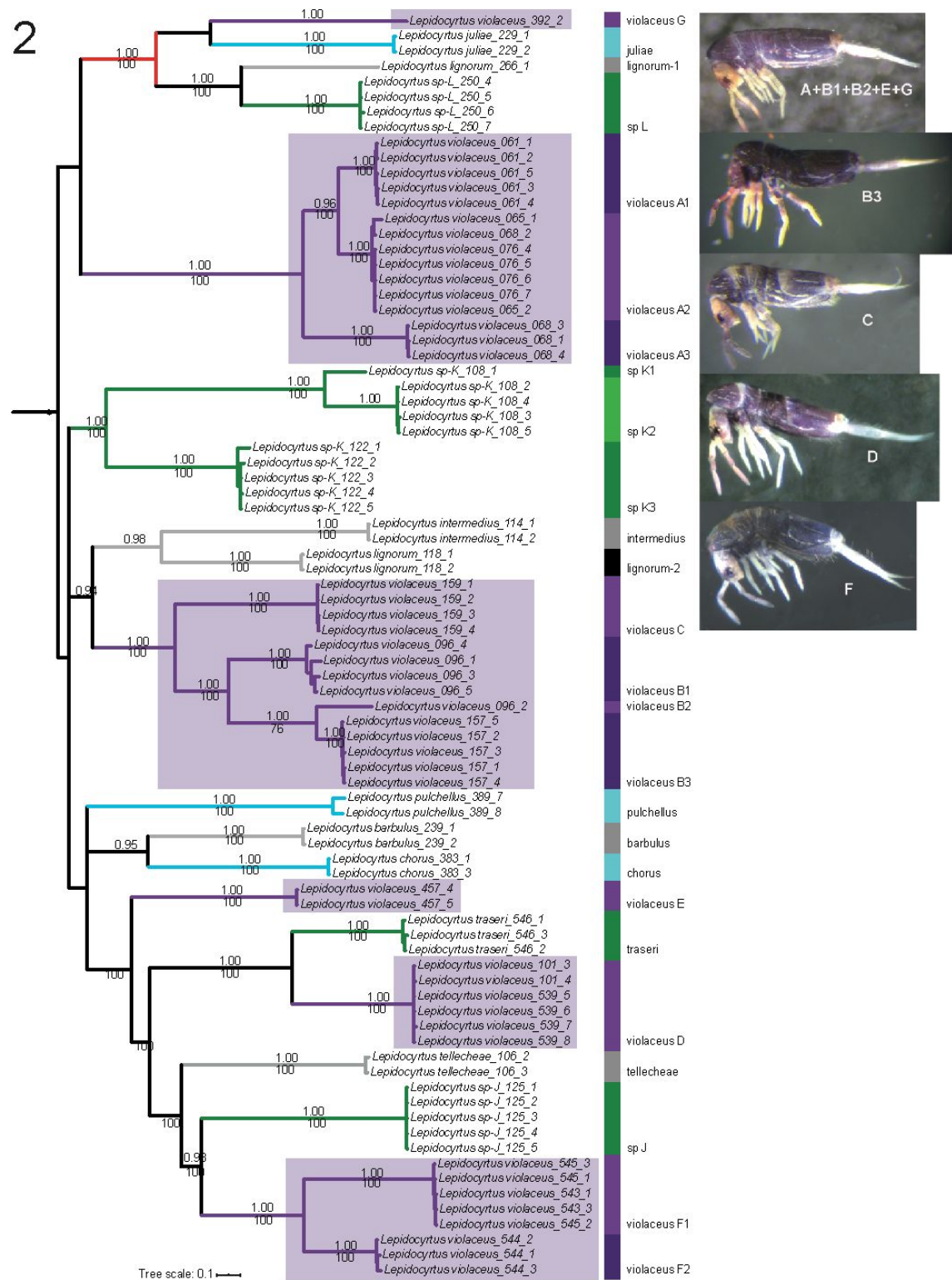
Table 4.

Body region	Position	Pos	#	A2	E	G
Legs	Cx.I	1	2	2	2	2
	Cx.II	2	4	4	4	4
	Cx.III	3	2	2	2	2
Head dorsal	Cephalic - exterior	4	1	1	1	1
	Cephalic - interior	5	2	2	2	2
Body dorsal	Th.II (mid dorsal)	6	1	1	1	1
	Th.III (mid dorsal)	7	1	1	1	1
	Abd.I (mid dorsal)	8	1	1	1	1
	Abd.II (mid dorsal)	9	1	1	1	1
	Abd.III (mid dorsal)	10	1	1	1	1
	Abd.IV (mid dorsal)	11	1	1	1	1
	Abd.IV (dorsal)	12	-	-	-	-
Furca dorsal	Manubrial base	13	2	2	2	2
	Manubrial plate	14	2	2	2	2
	Dentes	15	2	2	2	2
Ant. ventral	Ant.III	16	1	1	1	1
	Ant.II	17	1	1	1	1
	Ant.I	18	-	-	-	-
Body ventral	Th.I	19	1	1	1	1
	Th.II	20	1	1	1	1
	Th.III	21	1	1	1	1
	Abd.I - VT base anterior	22	1	1	1	1
	Abd.I - VT base posterior	23	1	1	1	1
	Abd.II	24	(3)	(3-4)	(4)	(3)
	Abd.III - post retinaculum	25	(2)	(2)	(2)	(2)
	Abd.IV	26	-	-	-	-
	Abd.V – pre genital plate	27	(1)	(1)	(1)	(1)
	Body lateral	Th.III	28	-	-	-
Abd.I		29	-	-	-	-
Abd.II		30	-	-	-	-
Abd.III		31	-	-	-	-
Abd.IV		32	-	-	-	-
BP4		33	-	-	-	7

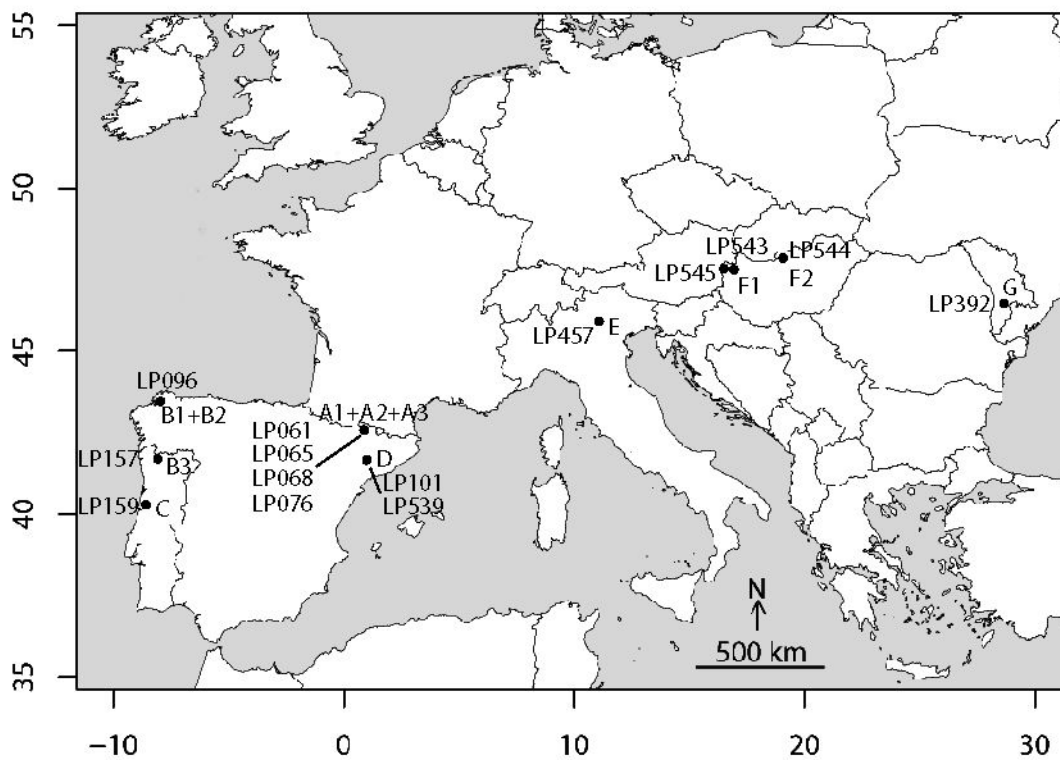
Table 5.

Sample Code	ABGD	N	Size	Ocular-q	Abd.II-mi	Abd.II-p5p	Abd.III-mi	Abd.III-d3	B4-B5/B5-B6	abd.IV-B6	BP4-pse
LP061	A1	6	1.3–1.5	-	-	-	-	+	1.23	bcM	-
LP065	A2	5	1.1–1.4	-	-	-	-	+	1.37	bcM	-
LP068	A2+A3	5	0.8–1.2	-	-	-	-	+	1.26	bcM	-
LP076	A2	5	1.3–1.6	-	-/+	-	-	+	1.18	bcM	-
LP096	B1+B2	2	1.0–1.2	-	-	-	-	+	2.03	tcM	-
LP157	B3	2	1.4–1.5	-	-	-	+	+	2.33	tcM	-
LP159	C	2	1.0–1.1	-	-	-	-/+	+	2.06	tcM	-
LP101	D	2	2.0	-	+	+	+	+	2.49	tcM	-
LP539	D	4	1.6–1.8	(-/+)	+	(-/+)	(-/+)	+	2.09	tcM	-
LP457	E	3	1.2–1.4	-	(-/+)	-/+	-/+	+	0.93	bcM	-
LP543	F1	1	1.3	-	-	+	-	-	2.18	tcM	-
LP544	F2	1	1.5	-	-	+	-	-	2.26	tcM	-
LP545	F1	1	1.0	-	-	+	-	-	2.35	tcM	-
LP392	G	1	1.1	-	-	-	-	-	1.11	bcM	+

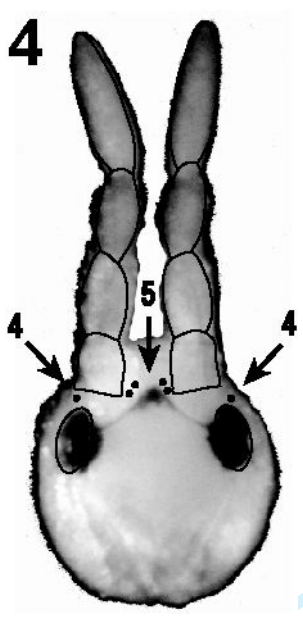




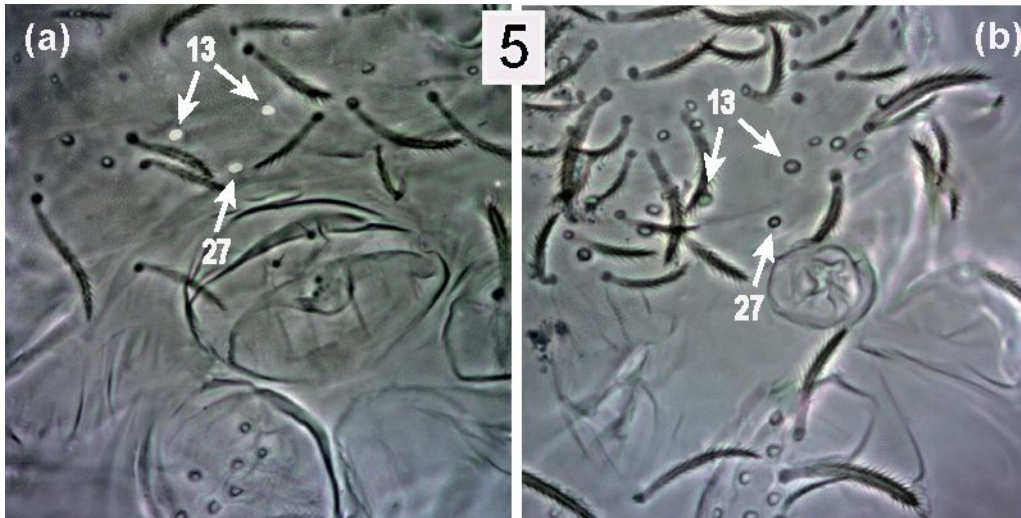
3



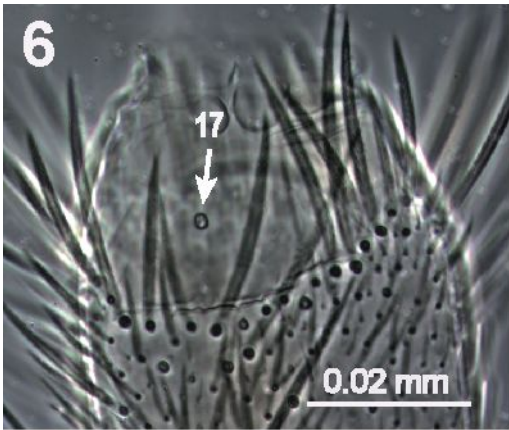
view Only



For Review Only



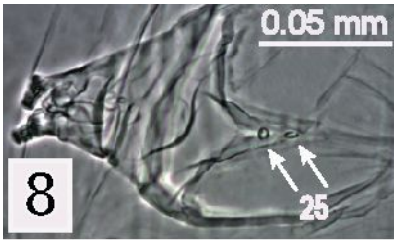
For Review Only



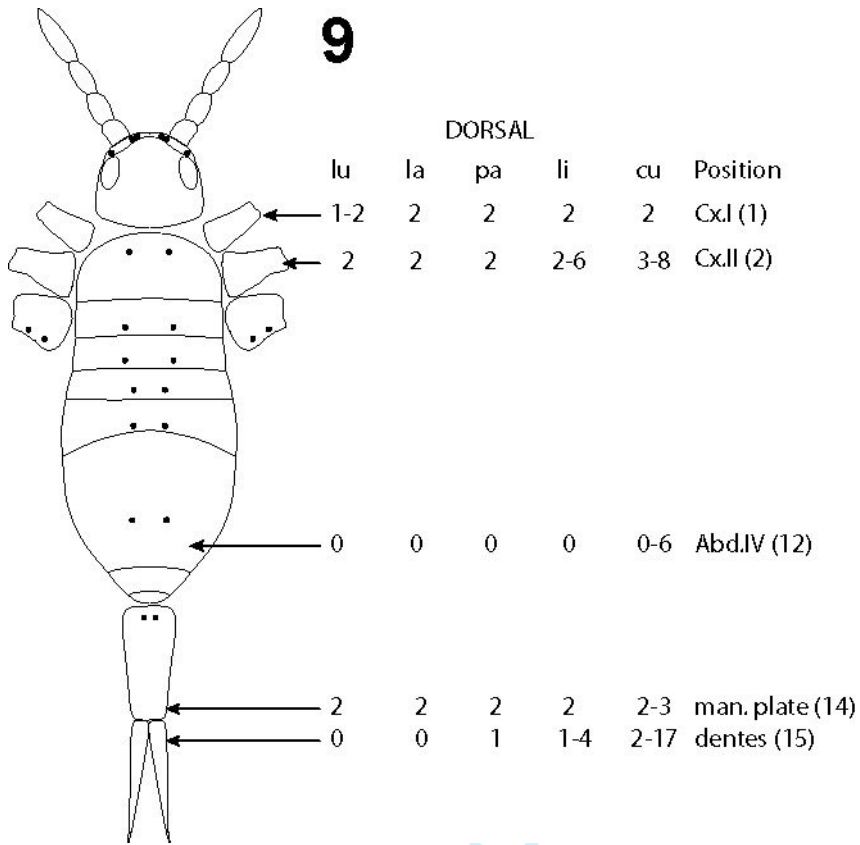
For Review Only



For Review Only

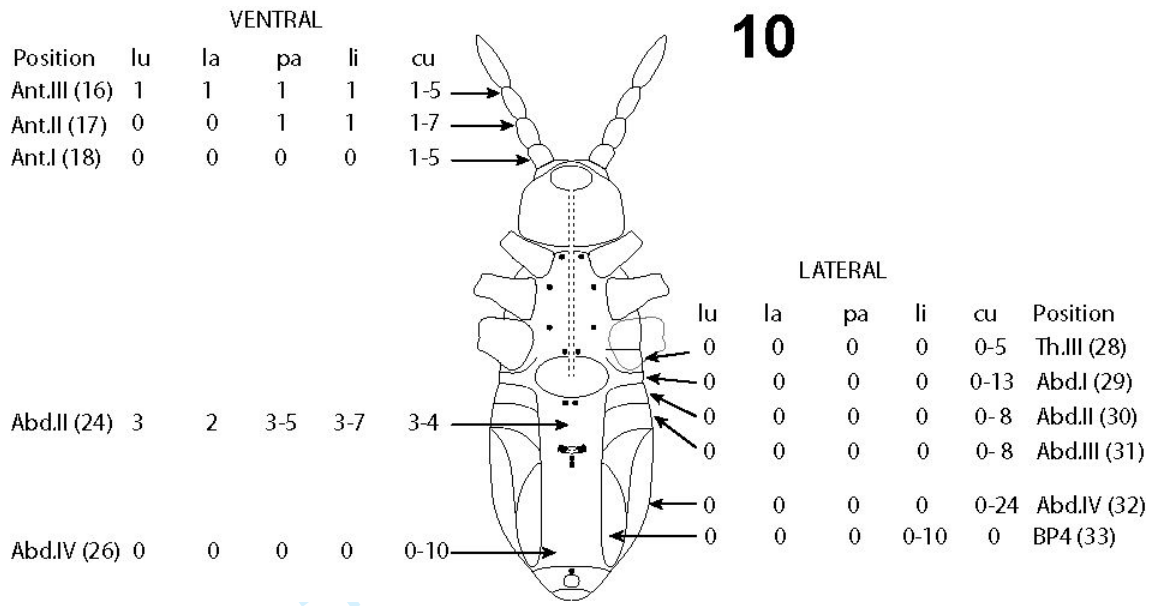


For Review Only

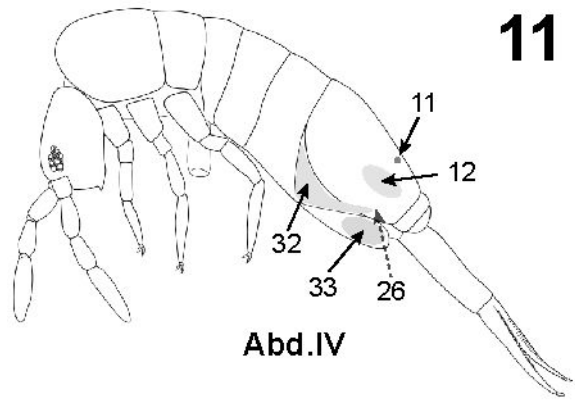


view Only

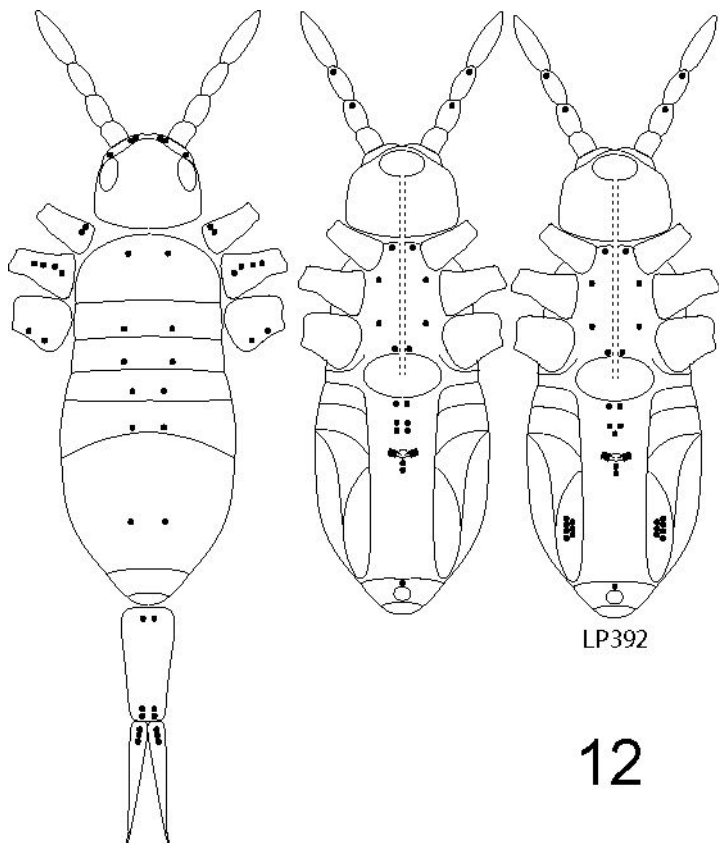
10



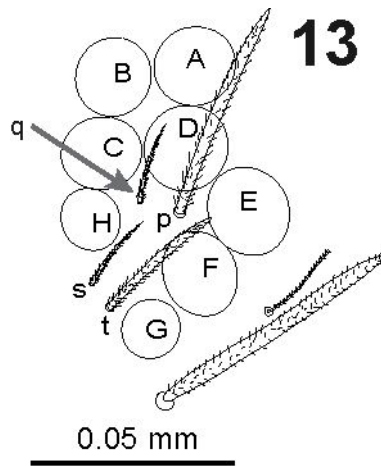
For Review Only



For Review Only

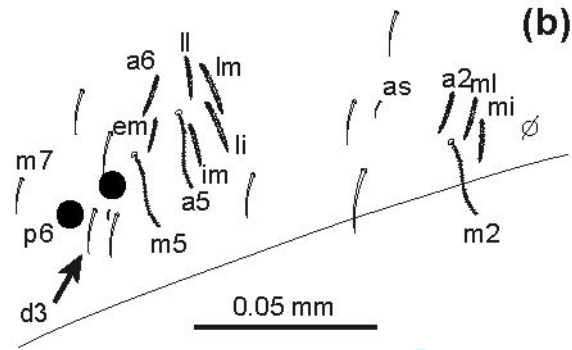
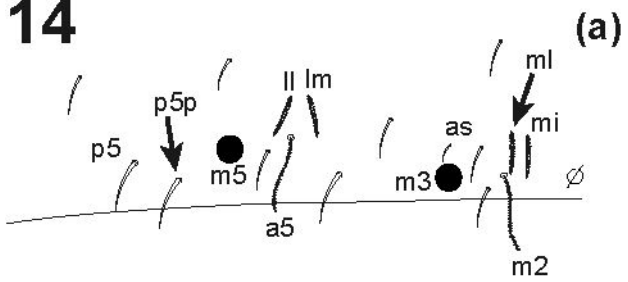


view Only



For Review Only

14



Review Only

15

